Advanced Energy Materials

ADVANCED ENERGY MATERIALS
www.advenergymat.de

REVIEW

In-Depth Knowledge of Strong Metal-Support Interaction Effect in Heterogeneous Catalysis

Ziyu Mei[1] | Miaomiao Xue[1,2,3] | Luyuan Wang[1,2,3] | Keren Wang[5] | Haozhen Dou[4] | Yuping Ren[1] | Yongguang Zhang[4] | Gaowu Qin[1] | Chuangwei Liu[2,3] | Yiwei Wang[5]

[1]Key Laboratory For Anisotropy and Texture of Materials, School of Material Science and Engineering, Northeastern University, Shenyang, China | [2]School of Software Engineering, Suzhou Institute for Advanced Research, University of Science and Technology of China, Suzhou, Jiangsu, China | [3]Key Laboratory of Precision and Intelligent Chemistry, School of Chemistry and Materials Science, University of Science and Technology of China, Hefei, Anhui, China | [4]State Key Laboratory of Catalysis, Dalian Institute of Chemical Physics, Chinese Academy of Science Dalian, Dalian, China | [5]Liaoning Province Key Laboratory For Phenomics of Human Ethnic Specificity and Critical Illness, Shenyang Medical College, Shenyang, Liaoning, China

Correspondence: Gaowu Qin (qingw@smm.neu.edu.cn) | Chuangwei Liu (liucw@ustc.edu.cn) | Yiwei Wang (wangyiwei@symc.edu.cn)

Received: 23 September 2025 | **Revised:** 7 November 2025

Keywords: design strategies | encapsulation | heterogeneous catalysts | strong metal-support interaction | support materials

ABSTRACT

Strong metal-support interaction (SMSI) in heterogeneous catalysts has received extensive attention because of its profound impact on interfacial stability and catalytic performance. With the rapid development of advanced characterization techniques and accurate theoretical calculations, remarkable progress has been achieved in elucidating the intrinsic nature of SMSI and in the rational reverse design of novel catalyst architectures. SMSI is characterized by several distinctive features, including the formation of protective encapsulation layers, significant electron transfer across the interface, and dynamic redispersion of metal species. Furthermore, strategies for constructing SMSI in various reactions are classified and discussed in detail to guide the development of new heterogeneous catalytic systems, providing valuable guidance for the design of efficient and durable catalytic systems. Finally, common research methods for SMSI catalysts are summarized from the perspectives of advanced in situ characterization techniques and theoretical modeling methods, which enable a deeper understanding of SMSI phenomena. To conclude, potential future research directions are outlined to overcome the current challenges and inspire the development of next-generation heterogeneous catalysts with enhanced activity, stability, and selectivity.

1 | Introduction

Catalytic technology serves as the cornerstone of the chemical industry, finding extensive application in over 50% of industrial reactions across various chemical sectors, as illustrated in Figure 1a. Although catalytic materials exhibit considerable diversity, more than 80% of industrial catalysts are predominantly represented as heterogeneous catalysts (Figure 1b), primarily due to their simplified process flows and cost-effectiveness in catalytic operations. The most prevalent type of heterogeneous catalyst, supported metal catalysts, is extensively utilized across various fields [1], including the chemical industry [2], waste treatment, and the design of advanced functional materials [3–5]. This widespread application is attributed to the unique interfacial chemical environment created by the active metallic species in their nanoscale structures, which are anchored onto the surface of the support material. The roles of supports in multiphase catalysts are remarkably diverse. They not only enhance the utilization efficiency of metal atoms and stabilize active metal species, but also participate directly in catalytic reactions [6–8]. On the other hand, the metal-support interactions (MSI) open up myriad possibilities for modulating catalytic

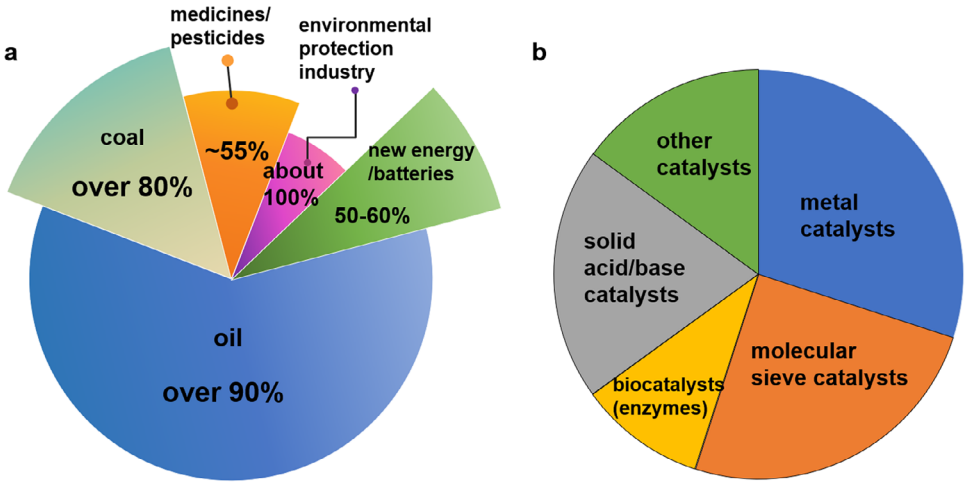

FIGURE 1 | (a) Schematic diagram of energy consumption ratio of major chemical processes. Percentage figures: usage ratio. (b) Schematic diagram of the application range of different forms of catalysts.

activity, selectivity, and stability. This interplay positions MSI as a profoundly intriguing scientific question, warranting extensive investigation to unlock deeper insights and transformative applications [9–12]. For instance, Li et al. investigated the sintering resistance of supported metal nanoparticles (NPs) and proposed a Sabatier principle: excessively strong metal-support interactions trigger Ostwald ripening, whereas overly weak interactions promote particle migration and coalescence. Consequently, metal-support binding energy serves as a descriptor to predict the growth kinetics of supported NPs under these competing mechanisms [13].

As a unique concept of MSI, strong metal-support interaction (SMSI) was first proposed by Tauster et al. in 1978 [14]. Group VIII noble metals (Pt, Pd, Ir, Ru, and Rh) supported on TiO_2 exhibited more uniform nanoparticles (NPs) dispersion at 200°C during the hydrogen reduction process, and the NPs structures were beneficial to small gas molecules (H_2, CO) adsorption in the initial step. However, the adsorption capacity of nanostructure quickly decreased to near-zero levels at 500°C [15, 16]. The reversible adsorption behavior of small gas molecules could be effectively regenerated through a treatment involving moderate-temperature oxidative reactivation followed by low-temperature reductive processing. Further characterization results revealed that this decrease in adsorption capacity was not caused by several known factors, such as nanoparticle aggregation, structural collapse of the support, or poisoning by impurities. To explain this phenomenon, Tauster introduced the concept of SMSI, attributing the reduced adsorption to chemical bonding between the metal species and TiO_2 surface atoms. Later studies proposed that the decreased adsorption of gas molecules might result from the encapsulation of metal nanoparticles by migrated TiO_x species, leading to the loss of exposed active metal sites. Although the root cause of the weakened adsorption of small inert gas molecules remained debated due to limitations in characterization techniques at the time, it became clear that modulating SMSI could effectively alter the geometric and electronic structures of metal nanoparticles, thereby influencing their catalytic performance [17, 18]. In 1986, Sakellson et al. provided direct evidence for the existence of the SMSI in Rh/TiO_2 using extended X-ray absorption fine structure (EXAFS) spectroscopy, specifically showing the presence of shorter Rh-Ti chemical bonds compared to those in Rh/Ti metal intermetallic compounds [19, 20]. However, constrained by the nascent stage of characterization techniques at that time, detecting the relatively low concentration of interfacial bonds within supported metal NPs remained challenging. Consequently, SMSI phenomena were further identified through macroscopic physicochemical manifestations, including encapsulation and diminished chemisorption capabilities. Subsequent studies have demonstrated that analogous SMSI phenomena manifest when other reducible metal oxides, such as CeO_2 [21, 22] and Nb_2O_5 [23], are employed as supports. Furthermore, these reduction-induced SMSI effects can be reversed through high-temperature oxidative treatment. Notably, recent advances have expanded the SMSI paradigm beyond conventional Group VIII noble metals (Pt and Pd) and reducible oxide supports, with emerging observations of such interactions in novel component systems [24]. The diverse geometric configurations across various SMSI systems provide expanded possibilities for constructing stable heterogeneous catalysts. In short, MSI is a ubiquitous interfacial effect that determines the dispersion and stability of metals. SMSI is a special form of MSI that dominates the dynamic reversible behavior and controllable catalytic performance of supported catalysts [25–27].

Deciphering the SMSI-activity relationship is imperative to improve the catalytic performance of catalysts and achieve inverse design of structure in heterogeneous reactions. Especially, it is essential to understand the reaction mechanism, critical role, and dynamic structure of SMSI involved systems during the dynamic heterogeneous catalytic process. Although some excellent and awesome works have been summarized the catalytic effect and development history of SMSI [28–30], they only enumerated the relationship between SMSI catalysts and experimental results. However, the dynamic catalytic main mechanisms and structural interface reconstruction during the reaction process on SMSI are summarized in this review thorugh the following key aspects: (1): Unique properties and structural design of SMSI; (2): SMSI research driven by advanced in situ characterization techniques and molecular dynamics simulation method; (3): Data-driven SMSI research paradigm for the next generation catalyst design. Therefore, a critical and

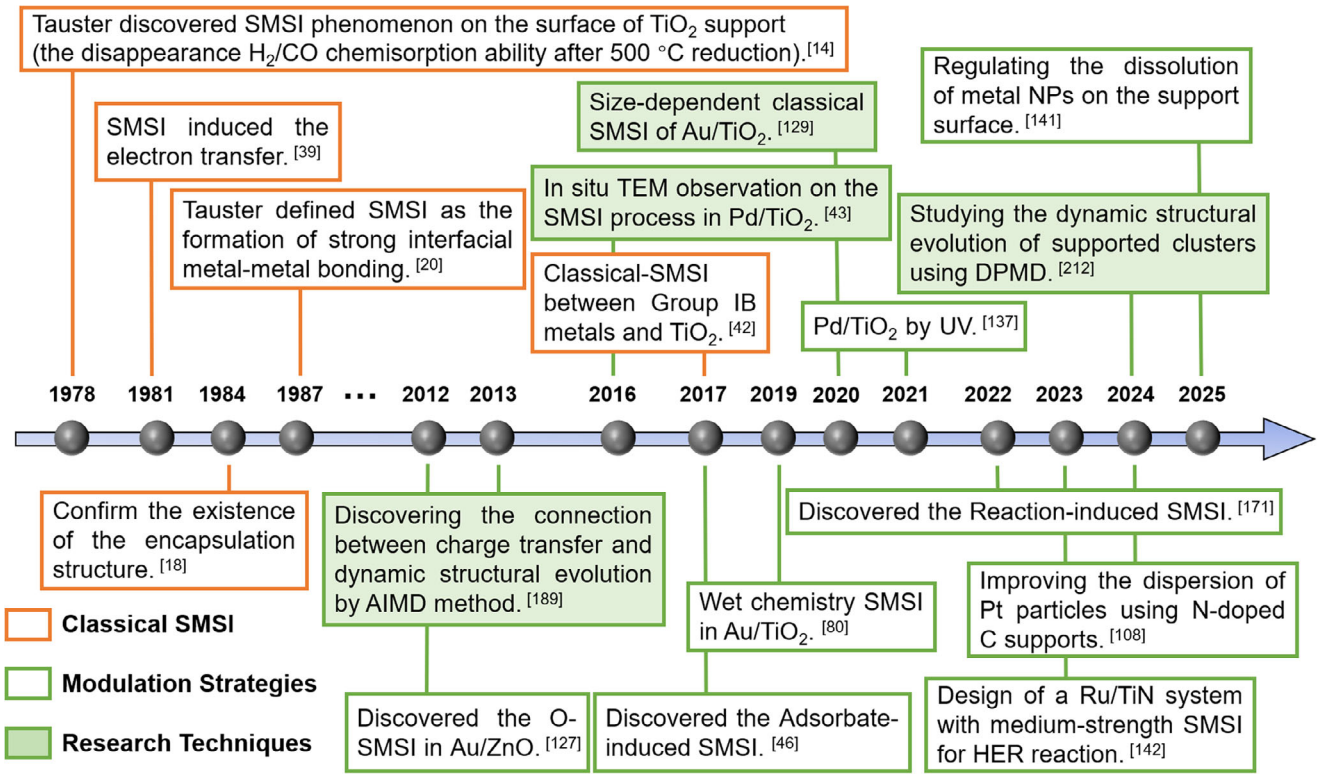

FIGURE 2 | The development journey of strong metal-support interaction.

systematic review of the fundamental characteristics and recent advancements in SMSI is both necessary and desirable for the comprehensive understanding and application of SMSI in heterogeneous catalyst development. In this review, we present the principles underlying both classical and emerging SMSI systems, broadening the comprehension of this unique phenomenon. The development path of SMSI is shown in Figure 2. The work systematically examines methodological approaches for investigating SMSI-related scientific debates and deciphering SMSI-activity relationship through experimental results, advanced characterization and theoretical computations. Furthermore, it discusses recent discoveries in SMSI engineering strategies and material systems, while comprehensively summarizing SMSI applications in controlling the activity, selectivity, and stability of heterogeneous catalysts. The review concludes with critical perspectives on remaining challenges and future opportunities in SMSI research.

2 | Key Types of SMSI

Beyond the pioneering observations by Tauster et al. [14], who reported a decrease in gas molecules adsorption, Burch et al. also found that after high-temperature reduction at 650°C, the adsorption of H_2 on Ni/TiO_2 significantly decreased [31]. Similarly, Golunski et al. observed that CO adsorption on Pt/CeO_2 was greatly reduced after reduction above 600°C [32]. In addition to hydrogen reduction, oxygen treatmentand the formation of adsorbate-induced SMSI states also weaken the adsorption of small molecules. These findings collectively demonstrate that suppressed small molecule adsorption is a typical feature of SMSI [33, 34]. Although early studies regarded weakened adsorptionas detrimental to catalytic performance, later investigations revealed that SMSI can in fact suppress undersired side reactions in several processes, including the selective hydrogenation of 3-nitrostyrene [35], dry reforming of methane [36], and the water-gas shift reaction [37].

Subsequent studies further revealed that SMSI involves not only material transport across the NPs/support interface (see Figure 3a–f) but also interfacial charge transfer/redistribution [38, 39]. To emphasize this distinction, the term Electronic Metal-Support Interaction (EMSI) was introduced. Metal-support bonding is often accompanied by electron transfer. Studies have shown that electron transfer between the metal and the support is not only a typical feature of SMSI but may also be an important factor triggering support migration [40, 41]. The driving force for electron transfer is the difference in work function(Φ) or Fermi levels (E_f) between the metal and the support. Electrons will flow from the surface with a higher Fermi level to the surface with a lower Fermi level, as shown in Figure 3h. Notably, despite the relatively low work functions and surface energies of noble metals such as Pd and Au, high-temperature hydrogen reduction promotes the formation of structural defects on support surfaces. These oxygen-deficient sites enhance interfacial electron transfer dynamics between the support and metallic components. This understanding of the mechanism has enabled researchers to successfully construct EMSI in many systems, such as Pd/TiO_2 and Au/TiO_2 systems [42, 43]. In addition to classical SMSI systems, electron transfer between the metal and support has also been observed in novel SMSI systems. For example, SMSI systems constructed through hydroxide transformation (Au/LDO) [44], O-SMSI systems constructed through high-temperature oxygen treatment (including Au/ZnO

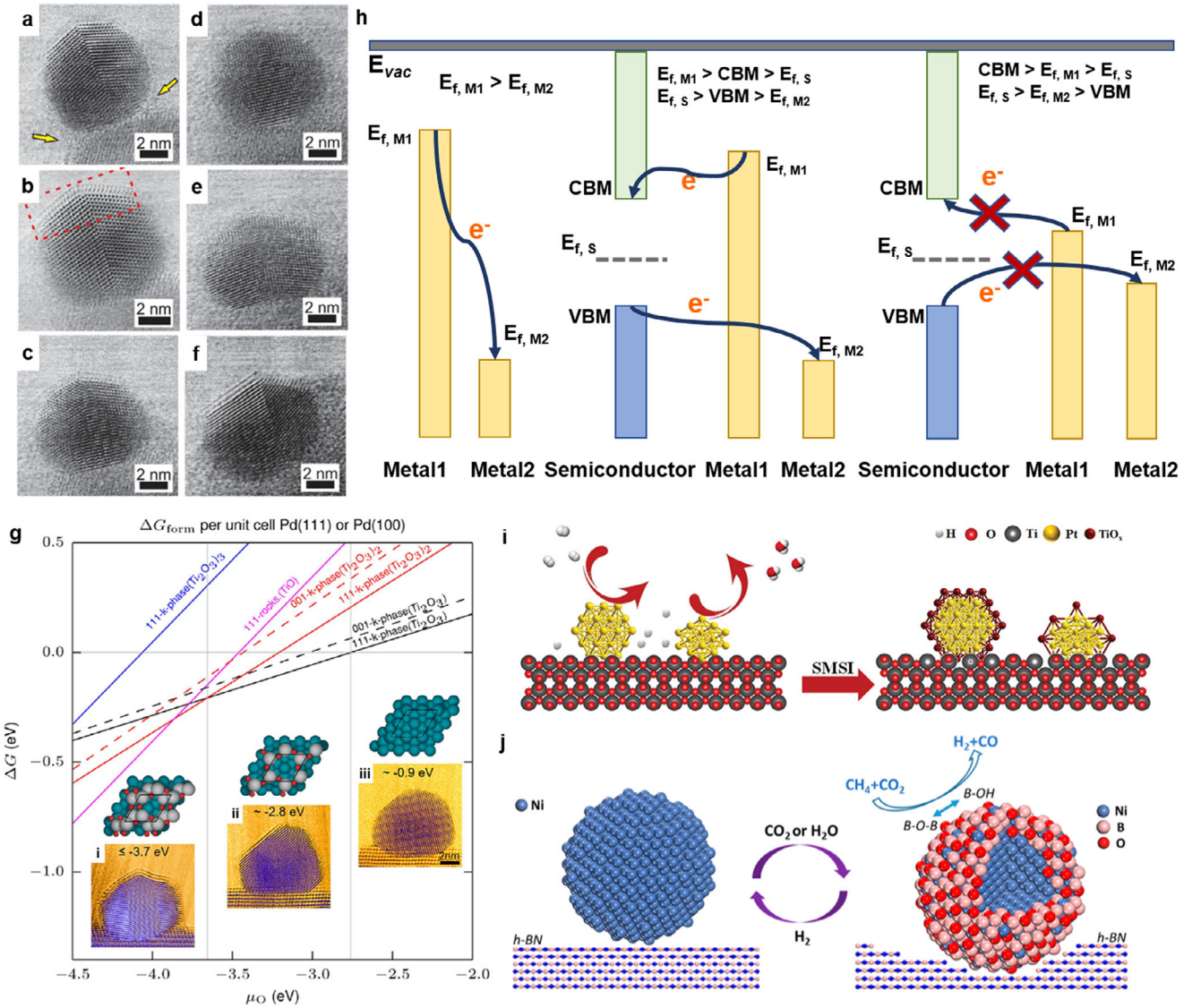

FIGURE 3 | (a–f) Reversible formation of the TiO_x overlayer on Pd nanocrystal in Pd/TiO_2. Sequential in situ observations: (a,b) under reducing conditions. (c–e) under oxidizing conditions. (f) under reducing conditions again. (g) Theoretical calculations of free energy G for different TiO_x phases on Pd(111) or Pd(100) surfaces as a function of oxygen chemical potential μ_o and characterization [43] Copyright 2016, American Chemical Society. (h) Schematic illustrations of electronic interfacial interactions occurring between adjacent components with different electronic structures. (i,j) Schematic diagram of encapsulated structures formation: (i) metal-metal bonds formation [28]. Copyright 2022, John Wiley and Sons. and (j) metal-oxide encapsulated structures [24]. Copyright 2020, American Chemical Society.

and Au/HAP) [45], A-SMSI systems constructed via adsorbates (Rh/TiO_2) [46], and SMSI systems induced by high-temperature carburization-air calcination (Au/TiO_2) [47]. In short, EMSI is a phenomenon that is widely present in heterogeneous catalyst systems. Researchers can construct the desired refined SMSI structures by regulating EMSI, which will be explained in detail in Chapter 3. Additional types of SMSI have been discovered and systematically categorized in Table 1. In general, the effects of SMSI under the different control methods mentioned in Table 1 can be divided into three categories: supported, encapsulated, and redispersed. In this chapter, we will introduce the relevant characteristics of SMSI according to these three categories to further explore the rational design of heterogeneous catalysts.

2.1 | Supporting Metal NPs

Supporting metal nanoparticles (NPs) involve dispersing metal NPs onto a stable solid material (the support) to improve their catalytic performance, stability, and recyclability in various chemical reactions, such as heterogeneous catalysis and fine chemical synthesis. The development of supported catalysts represents one of the most important achievements in heterogeneous catalysis, enabling industrial processes ranging from petroleum refining to environmental remediation and green energy conversion [48]. The concept of dispersing catalytically active species on high-surface-area supports was introduced to overcome the limitations of bulk catalysts, such as low surface utilization and rapid deactivation. By anchoring metals, oxides, or other active components

TABLE 1 | Overview of the different types of SMSI terminology. Abbreviations used in the table: Supported metal nanoparticles (SMNPs), supported metal clusters (SMCs), supported metal oxide nanoparticles (SMONPs), oxide metal inverse catalysts (OMICs), single atom catalysts (SACs).

Type of SMSI	Description	Catalyst system	Application	Reaction
Classic Strong Metal-Support Interaction (C-SMSI)	Mass migration from the support to encapsulate metal	SMNPs	Group VIII noble metals/TiO_2	Reduction at high temperatures
Electronic Metal-Support Interaction (EMSI)	Electron transfer occurs naturally upon contact between the metal and the support	SMNPs	Pt/TiO_2, metal clusters/oxides	CO oxidation
Oxidative Strong Metal-Support Interaction (O-SMSI)	O_2-treatment-induced SMSI	SMNPs	Au/ZnO	CO oxidation
Adsorbate-mediated Strong Metal-Support Interaction (A-SMSI)	Treatment under lower temperature in CO_2/H_2 atmosphere	SMNPs	Rh/TiO_2, Rh/ Nb_2O_5	Reverse water-gas shift reaction
Wet-chemistry Strong Metal-Support Interaction (WC-SMSI)	Interaction occurs at room temperature in a liquid environment	SMNPs	Au, Pt, Ru, Rh, and Pd with TiO_2	CO oxidation
Reactive Metal-Support Interaction (RMSI)	The metal reacts with the support to form an alloy phase	SMNPs	Pt/Nb_2CT_x MXene	Photocatalytic hydrogen production
Electronic oxide Metal-Support Interaction (EOMI)	Metal-to-oxide charge transfer (from metal substrates to supported MO adlayer), mainly on model catalysts where the metal is used as support	OMICs	CeO_x/Cu(111)	Hydrogenation of CO_2 to methanol
Electronic oxide Metal-Support Strong Interaction (EOMSI)	Metal-to-oxide charge transfer (from metal substrates to supported MO adlayer), formation of thin oxide adlayers containing low-valent metal cations	OMICs	CeO_x/Cu(111)	Water-gas shift reaction
Metal carbide-induced Strong Metal-Support Interaction (MC-SMSI)	Highly dispersed metal species on carbides are significantly positively charged	SMNPs	Pt, Ni, Co, Pd with α-MoC	Water-gas shift reaction
Covalent Metal–Support Interaction (CMSI)	Strong covalent bond formation, prevalent in single atom catalysts	SACs	Au_1/FeO_x	CO oxidation
Strong Electronic Oxide-Support Interaction (SEOSI)	Charge transfer from support oxide to oxide catalyst	SMONPs	In_2O_3/ZrO_2	CO_2 hydrogenation to methanol

onto suitable support materials, researchers have significantly enhanced activity, stability, and selectivity [4, 27].

Early supported catalysts were based on porous oxides such as silica, alumina, and carbon. These materials offered a large surface area that allowed fine dispersion of metal nanoparticles, maximizing the number of exposed active sites per unit mass of the catalyst [40, 49]. This dispersion effect remains one of the fundamental advantages of supported catalysts: a small quantity of precious metal can be dispersed into extremely fine clusters, achieving high catalytic efficiency while reducing material costs. For example, the introduction of alumina-supported platinum and palladium catalysts revolutionized petroleum reforming and automotive emission control by combining high dispersion with structural robustness [50, 51].

Beyond dispersion, the support also plays a critical role in stabilizing the active phase. Metal nanoparticles are inherently prone to aggregation or sintering under reaction conditions, which leads to a loss of active surface area. The interaction between the support and the dispersed species helps prevent this by anchoring the particles and limiting their mobility. After the SMSI concept was proposed, supported catalysts were further studied, and researchers revealed that the support can change the active phase in both electronic and structural manners, thereby affecting the catalytic performance. For instance, reducible oxides like TiO_2 and CeO_2 not only stabilize metal particles but also provide oxygen storage and transfer capabilities, enhancing reactions such as CO oxidation and hydrocarbon reforming [52, 53].

The development of supported catalysts has also evolved toward tailoring the chemical nature of supports. Rather than being inert supports, supports are now engineered to actively participate in reactions, provide acid-base functionalities, and promote synergistic effects. Zeolites, with their well-defined microporous structures, serve as both dispersive hosts and active participants, offering shape selectivity and confinement effects in reactions such as fluid catalytic cracking and methanol-to-olefin conversion. Similarly, mesoporous silicas and metal–organic frameworks have emerged as advanced supports with tunable porosity, surface chemistry, and metal-support interactions [54, 55]. Advances in synthesis, such as atomic layer deposition and colloidal methods, have allowed precise control over particle size, dispersion, and distribution on supports [56]. In modern catalyst design, supports have evolved from passive scaffolds to active components in catalysis. This dual functionality not only extends the life of catalysts but also opens avenues for improved efficiency, reduced costs, and more sustainable chemical processes. Therefore, the development of novel supports remains at the core of SMSI research efforts.

2.2 | Encapsulating Metal NPs

Encapsulating metal nanoparticles (NPs) involves surrounding them with a layer of another material to improve their stability, prevent aggregation, and enhance their catalytic performance. Since the SMSI concept was proposed by Tauster et al. in 1978, researchers have conducted extensive studies on its formation mechanism [57]. It is generally believed that one of the main driving forces behind SMSI formation is the surface energy difference between metal nanoparticles and the support, which induces the migration of the support material to the higher surface energy metal nanoparticle surface, thereby stabilizing the metal particles [58, 59]. Moreover, metal nanoparticles with high surface energy can effectively activate hydrogen to reduce the support surface, leading to the formation of a movable oxide thin layer that coats the metal nanoparticles. The encapsulation structure strongly influences catalytic performance. It can suppress undesirable reactions by selectively blocking certain sites, thereby improving selectivity. For example, the encapsulated metal often shows reduced activity for hydrogen chemisorption but enhanced resistance against sintering, resulting in improved stability under severe reaction conditions. On the other hand, the migration of support species may partially cover active sites, leading to decreased apparent activity in some reactions. This dual effect highlights the complex role of SMSI in tuning catalyst behavior. Recent advances in characterization techniques have confirmed that encapsulation is not a static phenomenon but a dynamic and reversible process. The overlayer can form under reducing conditions and disappear upon oxidation or reoxidation, offering opportunities for switchable catalysis. Moreover, by tailoring the chemical composition of the support and tuning the reduction environment, researchers can finely regulate the degree of encapsulation, thereby achieving a rational balance between catalytic activity, selectivity, and stability.

To elucidate the reversible nature and atomic-scale mechanism of SMSI, recent studies have increasingly employed in situ and operando characterization techniques. These advanced approaches enable direct visualization of structural and electronic transformations under reaction-relevant conditions, bridging the gap between theoretical predictions and dynamic experimental observations. Traditionally, SMSI formation has been considered to require high-temperature hydrogen treatment [20]. Using in situ environmental high-resolution transmission electron microscopy (HRTEM), Zhang et al. achieved the first real-time observation of SMSI formation in Pd/TiO_2 systems. As illustrated in Figure 3a–f, under 5 vol% H_2/Ar atmosphere, Pd nanoparticles initiated the formation of amorphous TiO_x overlayers at approximately 300°C. Upon heating to 500°C, these overlayers underwent progressive crystallization, while the Pd nanoparticles simultaneously restructured to minimize surface energy [43]. Notably, the encapsulating layers gradually dissolved when subjected to oxidative thermal treatment. Density Functional Theory (DFT) calculations shown in Figure 3g revealed that oxygen chemical potential governs the overlayer coverage extent, exhibiting temperature- and oxygen partial pressure-dependent characteristics. Subsequently, Bohkoven et al. combined advanced in situ TEM, XPS, and X-ray diffraction techniques to demonstrate Pt-Ti alloying at Pt/TiO_x interfaces following high-temperature H_2 treatment [60]. They speculated that in a high-temperature hydrogen environment, the d-orbitals of noble metal ions (such as Pt) overlap with the empty d-orbitals of Ti^{4+} ions, promoting the formation of metal-metal bonds. For example, in the reaction $TiO_2 + 2H_2 + 3Pt \rightarrow TiPt_3 + 2H_2O$, this type of bonding is thermodynamically and kinetically feasible, similar to the structure of hexagonal barium titanate. Subsequently, Horsley et al. used molecular orbital calculations to further study the Pt/TiO_2 system and proposed two models that supported the theoretical foundation for Pt-Ti bonding [61]. Additionally, researchers employed techniques such as XPS,

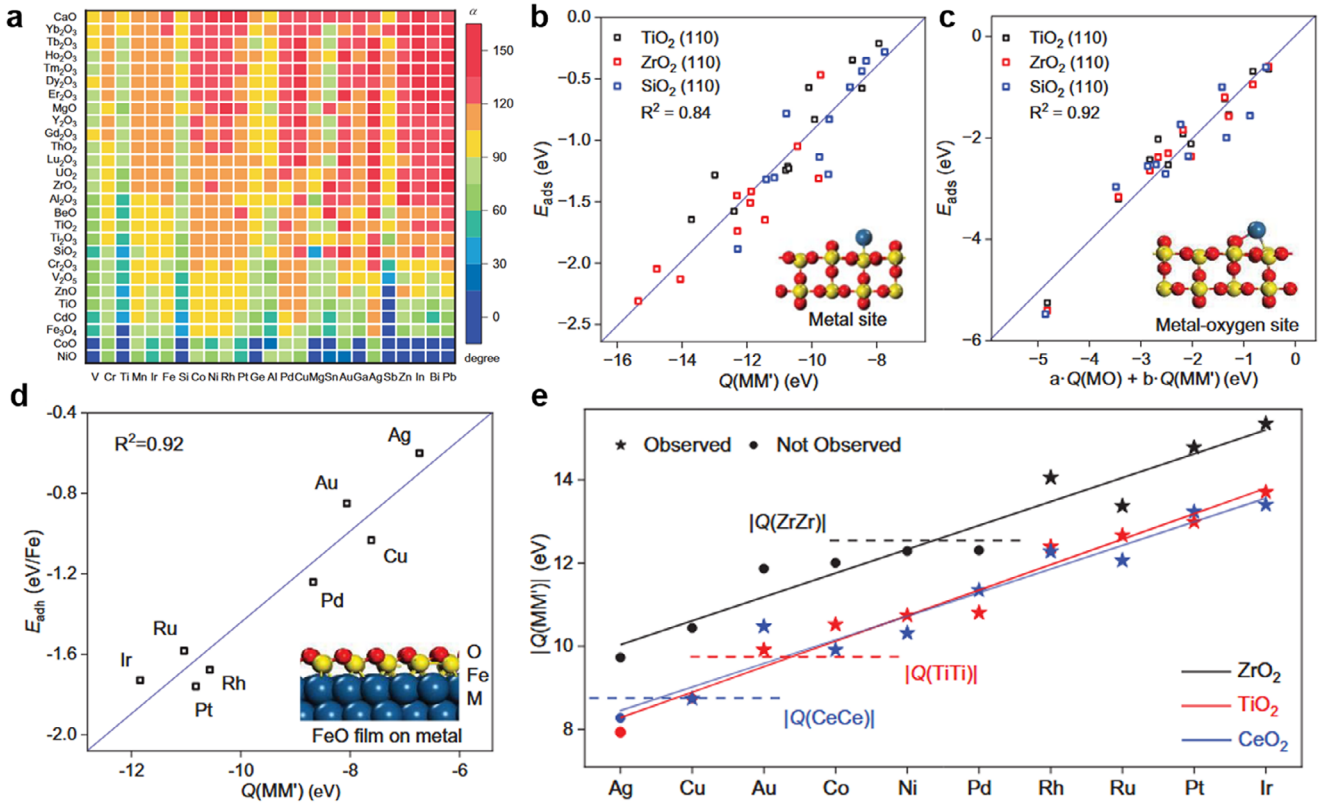

FIGURE 4 | (a) Predicting metal oxide interface contact angles using machine learning algorithms. (b,c) Linear fitting of adsorption energy E_{ads} and the interaction descriptor (Q) between b) metal atoms and metal sites and (c) oxygen sites. (d) Linear fitting of adhesion energy E_{adh} and Q(MM') to find encapsulated structure. (e) Q(MM') for late TMs with corresponding M' affinity of M' in oxide [13]. Copyright 2024, The American Association for the Advancement of Science.

AES, and TEM to discover that after high-temperature hydrogen treatment, low-valent Ti species formed on the surface of Pt/TiO_2 could enter the Pt lattice and interact with Pt to form metal-like intermetallic compounds or Pt-Ti microcrystals, which led to lattice expansion and distortion of Pt (see Figure 3i) [62–64]. These studies provided experimental evidence for metal-metal bonding. A representative study demonstrated this progress by employing controlled oxygen treatment at specific temperature ranges (200°C–400°C) to engineer a novel oxygen-mediated strong metal-support interaction (O-SMSI) structure on Au/ZnO supports. EXAFS analysis of Au's local coordination environment revealed distinct Au-Zn interfacial interactions forming at 60°C–200°C under oxygen atmosphere. Subsequent hydrogen reduction at 300°C enabled direct detection of Au-Zn chemical bonding, exhibiting structural characteristics analogous to intermetallic Au-Zn alloys. These findings demonstrate that the O-SMSI system retains intrinsic metal-metal bonding features at the interface, even under oxidative preparation conditions [65]. Non-metallic supports were also found to form similar encapsulation structures subsequently, as shown in Figure 3j. Li et al. recently used interpretable machine learning (SISSO) to confirm that the SMSI-induced wrapping structure is driven by the metal-support metal affinity (MMI), rather than the metal oxygen affinity (MOI). As shown in Figure 4a, data from 178 metal-oxide interfaces were calculated and generalized to 675 structures. The results show that weak MSI leads to larger contact angles and makes the catalyst more susceptible to sintering upon heating. Figure 4b–e confirms that MMI-dominated structures are more likely to form encapsulated structures. In general, the compositional design of each component of a heterogeneous catalyst is crucial for its stability and performance, a topic discussed in detail in the next chapter [13].

2.3 | Redispersing Metal NPs

Redispersing metal NPs involves breaking apart already aggregated metal NPs into their smaller clusters or individual atoms to maintain a stable, dispersed state, often within a liquid medium. Since Tauster et al. first proposed SMSI, subsequent studies have not only confirmed the encapsulation phenomenon but also revealed that redispersion is an equally important manifestation of SMSI. With the development of advanced in situ characterization techniques, such as transmission electron microscopy and X-ray absorption spectroscopy, the dynamic nature of redispersion has been directly observed and is now widely recognized as a fundamental mechanism in supported metal catalysts. Redispersion under SMSI generally refers to the transformation of aggregated metal NPs into highly dispersed species, including small clusters or even single-atom catalysts (SACs). [66–70] Numerous recent studies have demonstrated that SACs often serve as the true active sites in various reactions, whereas larger clusters and nanoparticles are less effective. The established SMSI provides a powerful means of regulating this structural evolution by tuning the balance between metal–gas and metal–support interactions. In this way, SMSI is not only a factor that influences stability

but also a driver of catalyst regeneration and rational interface construction.

Mechanistically, the redispersion process involves two key steps: (1) the generation of mobile metal atoms and (2) their subsequent capture by the support. The first step requires metal atoms to be detached or mobilized from larger particles, which is strongly affected by the reaction environment, including gas composition, atmosphere, temperature, and applied potential. The second step depends on the support, which provides anchoring sites to capture and stabilize the mobile atoms, preventing reaggregation. Through this two-step mechanism, metals can be redistributed into more finely dispersed forms, often resulting in enhanced catalytic efficiency and improved atom utilization. An additional fascinating aspect of SMSI-driven redispersion is the reversible structural interconversion between SACs and clusters. Depending on external conditions such as gas atmosphere, coordination environment, and temperature, SACs can agglomerate into clusters under reducing conditions, while clusters may redisperse into SACs under oxidizing or reactive environments. This dynamic flexibility reflects the adaptive nature of supported catalysts and explains their capacity to maintain activity under fluctuating reaction conditions. Such reversible transformations also highlight why in situ or operando studies are essential for fully understanding catalyst behavior, as static ex situ characterizations often fail to capture these dynamic processes [71, 72]. The consequences of redispersion are profound. First, it provides a pathway for catalyst regeneration, allowing deactivated or sintered catalysts to recover high activity through controlled treatments. Second, it promotes the formation of highly dispersed metal species, which are desirable for maximizing catalytic efficiency, especially when using precious metals such as Pt, Pd, or Rh. Third, it introduces opportunities for "switchable catalysis," in which the structure of the catalyst can be deliberately altered by adjusting operating conditions to achieve different functionalities.

For example, in the Pt/CeO_2 or TiO_2 system, Pt single atoms exist stably in an oxidizing atmosphere, while during CO oxidation, Pt SACs may dynamically evolve into Pt cluster structures in a H_2 or CO + O_2 mixed atmosphere [73]. Li and Zhang observed that after continuous high-temperature hydrogen reduction-oxidation treatment, the CO adsorption ability of the Au/TiO_2 system could decrease and recover reversibly, as determined by in situ CO adsorption DRIFTS [42]. At the same time, the negative charge on the surface of the Au nanoparticles decreased. Li et al. engineered cation vacancies at the Al_2O_3-La_2O_3 interface by stimulating interfacial reconstruction driven by strong oxide-support interactions during calcination, thereby inducing the redispersion of Pt NPs to form Pt single atoms, as shown in Figure 5a,b. DFT calculations showed that the introduction of La_2O_3 simultaneously promoted the formation of cation vacancies and suppressed the evaporation of Pt single atoms, as shown in Figure 5c,d [74]. Recently, it has been demonstrated that the redispersion of metal NPs from oxides to carbides/nitrides provides a new approach for designing catalysts by tuning the number and properties of dual interface sites. For example, the C_xN_y supported Cu single atoms undergo dynamic structural evolution into clusters under negative potentials, induced by hydrogen adsorption. This process facilitates the generation of C_2H_5OH and NH_3 intermediates during NO_3^- and CO_2 [75, 76] reduction reactions (NO_3RR and CO_2RR). Additional studies reveal that other transition metals, rare earth metals, and noble metal clusters may also experience dynamic structural evolution under pyrolysis conditions. These clusters can transform into small molecular species that are subsequently captured by adjacent N-doping sites, forming thermodynamically stable M-N-C structures [77]. In certain noble metal systems, different gas atmospheres can induce similar dynamic behaviors. Currently, researchers can design specific reaction pathways for catalytic systems by understanding the dynamic evolution behavior patterns, thereby avoiding the formation of byproducts.

In summary, while encapsulation is a feature of SMSI, redispersion represents its complementary dimension, emphasizing the dynamic and reversible restructuring of supported metals. Through the delicate control of metal mobility and support anchoring ability, SMSI enables the redistribution of metals into atomically dispersed forms, leading to improved efficiency, tunable selectivity, and extended catalyst lifetime. Thus, redispersion under SMSI is not only a regeneration mechanism but also a central principle for the rational design of next-generation supported catalysts.

3 | Modulation Strategies and Inverse Design

Catalyst stability encompasses both the resistance to deactivation and the ability to undergo potential regeneration procedures after deactivation occurs. Deactivation is typically induced by one or a combination of three general mechanisms: first, the loss of active species through sintering, leaching, or promoter depletion; second, the blockage of active sites via poisoning or coke deposition; and third, the modification of active sites through phase transformations. [78] All these mechanisms are influenced to varying extents by different types of metal-support interactions, which should be ideally accounted for during catalyst design. Various metal-support interaction phenomena, such as charge transfer and the formation of specific metal-support encapsulation structures, have been systematically reviewed in the preceding sections. Currently, multiple strategies have been identified to modulate MSI, as illustrated in Figure 6. These include tuning the properties of the support (e.g., composition, morphology, and surface modification) and the metal (e.g., size and composition), as well as altering pretreatment conditions, all of which will be discussed in detail in this chapter [79, 80].

3.1 | Active Metal

The bonding between active metal (AM) atoms and non-reducible, defect-free supports predominantly involves covalent interactions, while reducible supports enable both covalent and ionic bonding configurations. Catalytically critical parameters are determined by the ratios of surface-exposed AM atoms (R_{surf}, representing dispersion) and interface-bound AM atoms (R_{int}) relative to the total AM content. As particle size decreases from bulk nanoparticles to single atoms, R_{surf} and R_{int} values progress from nearly 0 to 1. A higher R_{surf}/R_{int} ratio indicates an increase in the accessible atomic sites of the multiphase catalyst to reactants, while simultaneously intensifying the under-coordinated state of the AM and amplifying electron perturbation from the support (see Figure 7a,b).

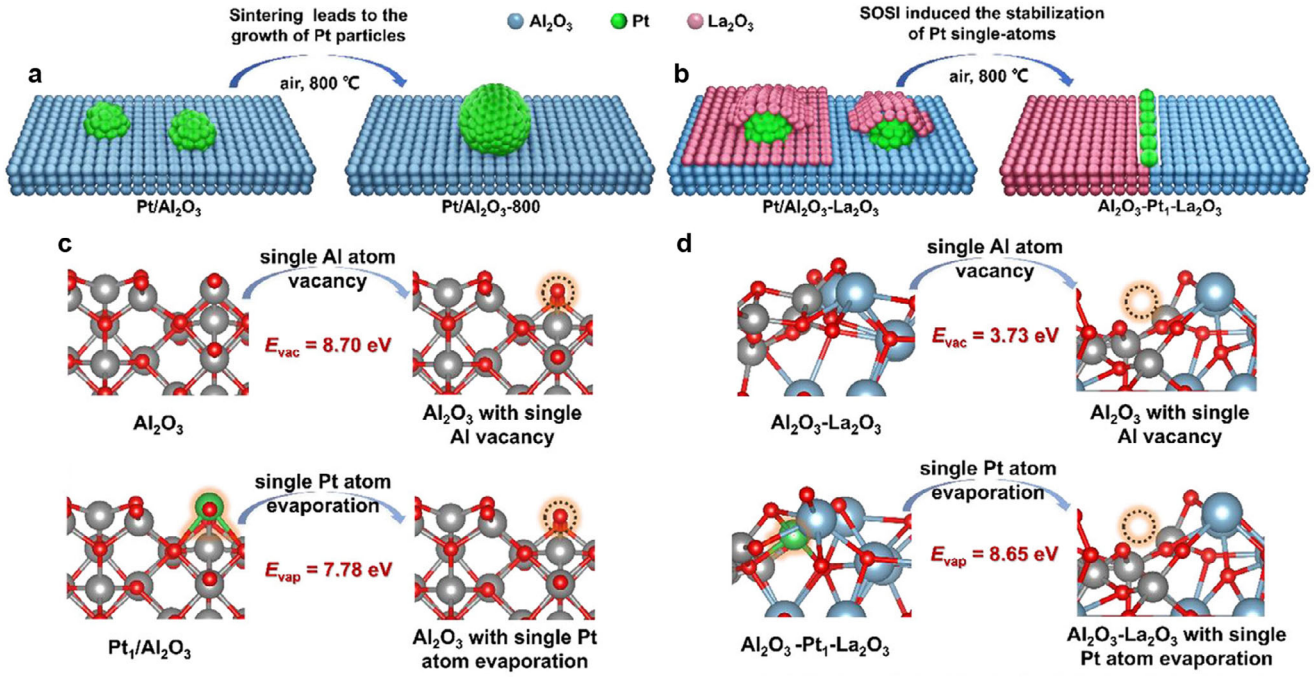

FIGURE 5 | (a,b) Schematic diagram of single-atom formation driven by strong oxide-support interaction (SOSI). (c,d) DFT results about cation-vacancy formation and Pt evaporation process of Pt_1-Al_2O_3 and Al_2O_3-Pt_1-La_2O_3 [74]. Copyright 2025, John Wiley and Sons.

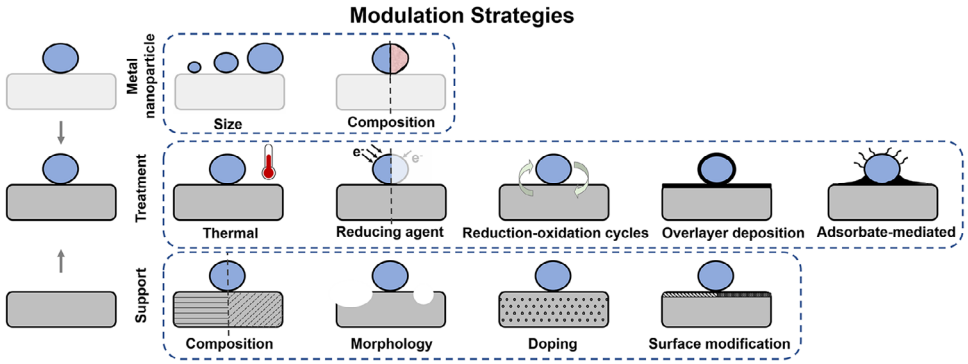

FIGURE 6 | Schematic illustrations of approaches for tuning the MSI at different stages of catalyst modifications.

In catalytic systems, metal nanoparticles exhibit polarization effects at metal/support interfaces dictated by the differences in energetics of metal and support used. Conversely, isolated AM atoms function as 0D point defects in the support, where the difference between the band edge and the AM state affects the binding energy with reactants and intermediates, and thus catalytic properties. The strength and nature of the interactions between AM and support are particularly significant when R_{surf} and R_{int} values are much smaller than 1. Under these conditions, the catalytic behavior of AM species becomes highly sensitive to the type of interaction they have with the surface, for example the defect-specific coordination environments at anchoring sites; the bonding character (covalent or ionic) and local electrostatic interactions with the support's cations/anions. Adsorbate interactions with surface AM atoms exhibit fundamental differences across elementary reaction steps, governed by the orbital hybridization mechanism. s-orbital dominated bonding preferentially activates undercoordinated sites (prevalent at R_{surf} close to 1), while p-orbital interactions favor more coordinated configurations. Enhanced surface interactions can stabilize transition states through orbital rehybridization, facilitating bond cleavage. For metal-support heterogeneous catalysts, the metal component typically assumes part of the catalytic reaction responsibilities. Therefore, regulating metal clusters or nanoparticles can directly influence SMSI, thereby improving the catalytic activity of the reaction.

The concept of catalysis with precise numbers of atoms emerged in the 1990s, motivated by the pursuit of understanding the unique properties and catalytic reactivity of nanoscale AM species [81]. Initial investigations employed mass-selection techniques to achieve precise control over the size distribution of AM clusters in the gas phase. Subsequently, a soft-landing approach was developed to deposit these gas-phase ions onto substrates with controlled kinetic energy, thereby preserving their original atomic configurations [82, 83]. With the advancement of this field, emerging strategies have brought novel perspectives to the design of supported cluster catalysts. These materials, termed

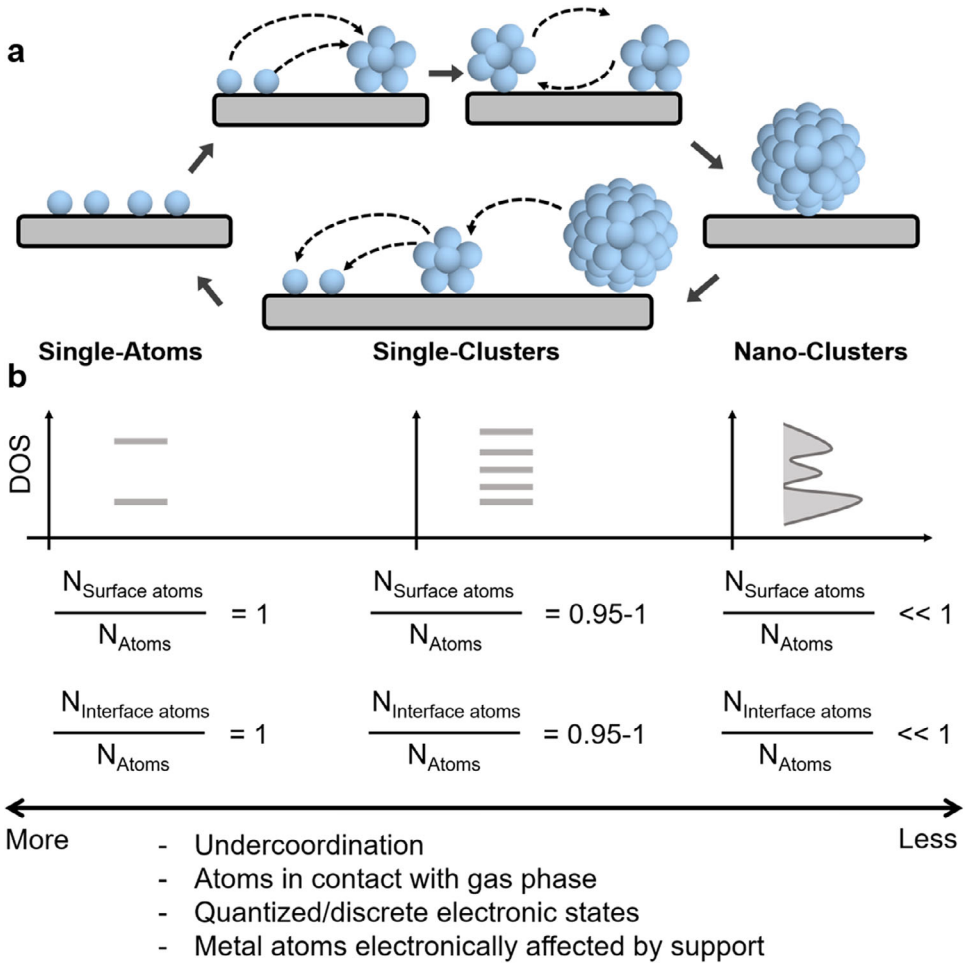

FIGURE 7 | Schematic diagram of the geometric structure and electronic structure of single atom, single cluster, and nano cluster catalysts.

single-cluster catalysts (SCCs), consist of atomically precise and isolated metal clusters (ranging from 2 to 20 atoms) anchored on suitable substrates. SCCs represent an intermediate category between heterogeneous single-atom catalysts (SACs) and conventional metal nanoparticle catalysts (NPs), the latter of which generally exhibit size distributions without atomic precision. Sub-nanometer metal clusters demonstrate distinctive physical and chemical properties arising from quantum size effects, electron confinement effects, and orbital hybridization of atomic clusters. These metal clusters possess discrete molecular orbital energy levels that can be systematically modulated between the continuous band structure of bulk metal particles and the discrete atomic orbitals characteristic of SACs with specific support interactions [84]. This tunability enables precise control over properties such as energy level alignment and electron affinity. The properties of the AM phase, such as electronic structure, morphology, and active site density, are affected by many factors, such as the type of AM and support, specific MSI, and the presence of ligands [85].

Zhang et al. reported that the size of Au nanoclusters in the Au/TiO_2 system affects the sensitivity of SMSI, providing new insights into regulating SMSI [86]. As shown in Figure 8a–i, Au NPs of ca. 5 nm are more facile to undergo Au/TiO_2 SMSI than those of ca. 2 nm. Kwak et al. observed analogous phenomena in Rh/TiO_2 [87] and Pd/Al_2O_3 [88] catalysts. Meanwhile, literature reports on CO_2 hydrogenation reactions [89–92] have documented size-dependent effects influencing reaction selectivity: entities such as individual atoms and clusters tend to preferentially generate CO, whereas larger particles exhibit enhanced H_2 activation capability and a higher propensity for CH_4 formation. Figure 8j shows a strong correlation between the catalytic reverse water-gas turnover frequency (TOF) and the ratio of Rh_{iso} sites and between the catalytic methanogenic TOF and the ratio of Rh_{NP} sites. Additionally, isolated atoms on the same support and nanoparticles of the same metal can exhibit distinctly different catalytic selectivities in competing parallel reaction pathways, and the disintegration of nanoparticles under reaction conditions can play an important role in controlling stability. The aforementioned findings substantiate the critical role of metal particle dimensions in modulating SMSI and steering reaction selectivity. However, under practical reaction conditions, catalysts can dynamically restructure owing to the differential stability of metal nanoparticles and the occurrence of SMSI during catalytic operation. Notably, Xin et al. demonstrated that under CO_2 hydrogenation conditions, precise control of ruthenium nanoparticle growth by modulating reaction temperature-coupled with regulated SMSI encapsulation induced by defective MoO_{3-x} overlayers-resulted in a remarkable shift in product selectivity from 100% CH_4 to over 99.0% CO [93].

The metastable nature of supported metal nanoparticles renders them prone to sintering, which poses significant constraints on

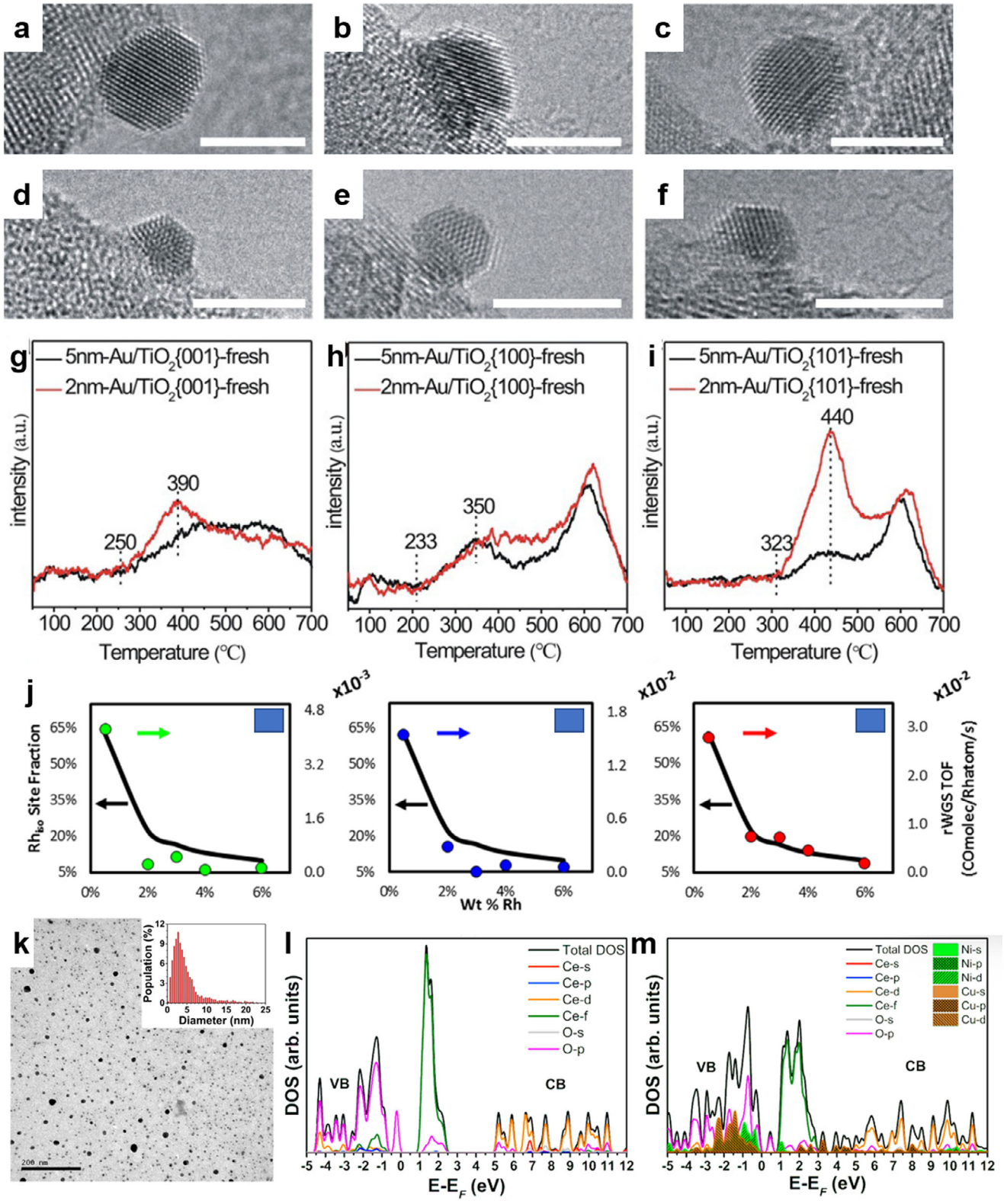

FIGURE 8 | (a–c) Representative HRTEM images of 5 nm-Au/TiO_2. (a) (001); b) (100); (c) (101). (d–f) Representative HRTEM images of 2 nm-Au/TiO_2. (d) (001); (e) (100); (f) (101). (g–i)H_2-TPR profiles [86]. Copyright 2021, John Wiley and Sons. j) Rh_{iso} site fraction and TOF plotted as a function of wt% Rh at CO_2:H_2 feed ratios = 1:4, 3:1, 10:1 [89]. Copyright 2015, American Chemical Society. (k–m) TEM and DOS images of bimetallic nanoparticles [94]. Copyright 2019, American Chemical Society.

their application in high-temperature heterogeneous catalysis. A strategic approach to circumvent these thermodynamic limitations inherent to reducible oxide supports involves encapsulation through SMSI. The dimensional attributes of nanoparticles may critically influence sintering tendencies and potential alloying behavior, where optimal particle size regulation could mediate the dynamic equilibrium between structural degradation and SMSI-induced stabilization. Lu et al. synthesized a series of Pd/ZnO catalysts using atomic layer deposition (ALD) technology, with Pd particle sizes ranging from 1.6 to 7.9 nm. Under high-temperature H_2 reduction, the Pd/ZnO catalysts exhibited a size-dependent SMSI effect, where larger Pd particles were more easily encapsulated by ZnO compared to smaller ones [95]. Additionally, Kaiser et al.'s study on the sintering stability of Pt clusters (Pt_5, Pt_{10}, Pt_{19}) supported on Fe_3O_4 revealed that all clusters exhibited encapsulation, coalescence, and Ostwald ripening upon gradual heating to 1073 K, ultimately forming single-crystalline Pt particles with cubic morphology. Notably, while these structural transformations occurred independently of the initial cluster size, the critical transition temperature was strongly dependent on the cluster dimensions [96].

The introduction of heteroatoms into SCCs creates adsorption sites with distinct properties, providing a valuable strategy for modulating reaction activity patterns. Heteroatom dopants can donate or extract electrons from metal clusters to regulate their electronic properties [97–99]. Numerous heteronuclear SCCs composed of different metal atoms have been synthesized for electrocatalytic applications, including hydrogen evolution reaction, oxygen evolution reaction, oxygen reduction reaction, carbon dioxide reduction reaction, and nitrogen reduction reaction. Some studies suggest that synergistic effects may exist between heteroatoms and metal centers, potentially correlated with their electronic structures.

For certain systems, a single metal is insufficient to induce a distinct SMSI. Figueiredo et al. synthesized Cu_xNi_{1-x}/CeO_2 ($0< x \leq 1$) nanoparticles and used them for the reverse water-gas shift (RWGS) reaction [94]. As shown in Figure 8k–m, studies of the nanoparticle surfaces indicated that their composition directly affected their reactivity. During the RWGS reaction, Ni atoms migrate to the surface of the nanoparticles. Nanoparticles that exhibited the SMSI effect (Cu-rich nanoparticles) displayed a Ni-enriched surface, which negatively impacted their reactivity toward CO_2 dissociation. The SMSI effect was responsible for closing off the catalytic active sites on the surface of the nanoparticles through a covering layer from the surrounding support, thereby decreasing their reactivity toward CO_2 dissociation. The density of states (DOS) calculations shown in Figure 8l evidenced the SMSI between NPs and supports. When Cu_2Ni_2 clusters are included (Figure 8m), the 4p orbitals of Cu and the 3d orbitals of Ni interact with the 4f orbitals of Ce, causing them to split. The valence band of CeO_2 to move toward the Fermi level, and electrons are transferred from the support to the active metal.

For certain complex reactions, the composition of the metal component can directly promote the reaction. Li et al., demonstrated that the origin of selective non-oxidative methane conversion on titanium carbide-supported nickel clusters lies in the formation of nickel carbide sites under reaction conditions [100]. These sites stabilize CH_x intermediates, facilitating C—C coupling. Additionally, computational studies confirmed that the formation of CH_x—CH_3 represents a key intermediate step in the reaction, providing new insights for the design of heterogeneous catalysts.

3.2 | Support

The AM clusters are typically anchored to the support through covalent bonds and electrostatic interactions. Engineering supports with desired properties can modulate the geometric, electronic, and catalytic characteristics of AM clusters [101]. Obtaining atomic-level insights into the chemical bonding configurations between AM clusters and their supports constitutes a prerequisite for establishing structure-property relationships in SCCs. Altering the properties of the support provides numerous possibilities for regulating interfacial interactions and is one of the commonly used strategies for SMSI modulation. Among various supports, oxides, carbon-based materials, and porous frameworks are the most representative categories; each exhibits distinct physicochemical properties that tailor catalytic behavior.

Oxides (such as TiO_2, Al_2O_3, and SiO_2) are the most widely used because of their structural and functional integration characteristics. For example, TiO_2 is notable for its reducibility and its ability to induce SMSI, which enhances catalyst stability and allows modulation of the electronic structure, making it ideal for reactions such as CO oxidation and hydrogenation. Al_2O_3 possesses a high surface area and excellent thermal stability, characteristics that make it indispensable for industrial hydroprocessing catalysts operating under harsh conditions. In contrast, SiO_2 is chemically inert and exhibits weak MSI, providing a neutral environment that minimizes electronic perturbation of the active metal sites, which is advantageous for studying intrinsic catalytic properties [102].

Carbon-based supports, including activated carbon, graphene, and carbon nanotubes, are valued for their high conductivity, large surface area, and adjustable surface chemistry. These features make them particularly suitable for electrocatalysis and energy-related processes where efficient electron transfer is required. Moreover, their tunable surface chemistry allows the anchoring of single atoms or small clusters, contributing to the design of highly dispersed active centers. Porous materials, such as zeolites and mesoporous silicas, constitute another important category. Their uniform pore structures and tunable acidity provide shape-selective catalytic environments, which are essential for petrochemical reactions such as cracking, isomerization, and methanol-to-olefins conversion. The confinement effect within the pores can also prevent sintering of metal particles, thereby enhancing catalyst durability. In recent years, hybrid and composite supports that integrate oxides, carbons, and porous frameworks have attracted increasing attention. These multifunctional materials combine structural stability, electronic tunability, and high surface accessibility, offering new opportunities for rational catalyst design that achieve an optimal balance between activity, selectivity, and stability across diverse reaction conditions.

The primary consideration is the chemical environment of the support, with key influencing factors including the surface microstructure of the support (e.g., oxygen vacancies and

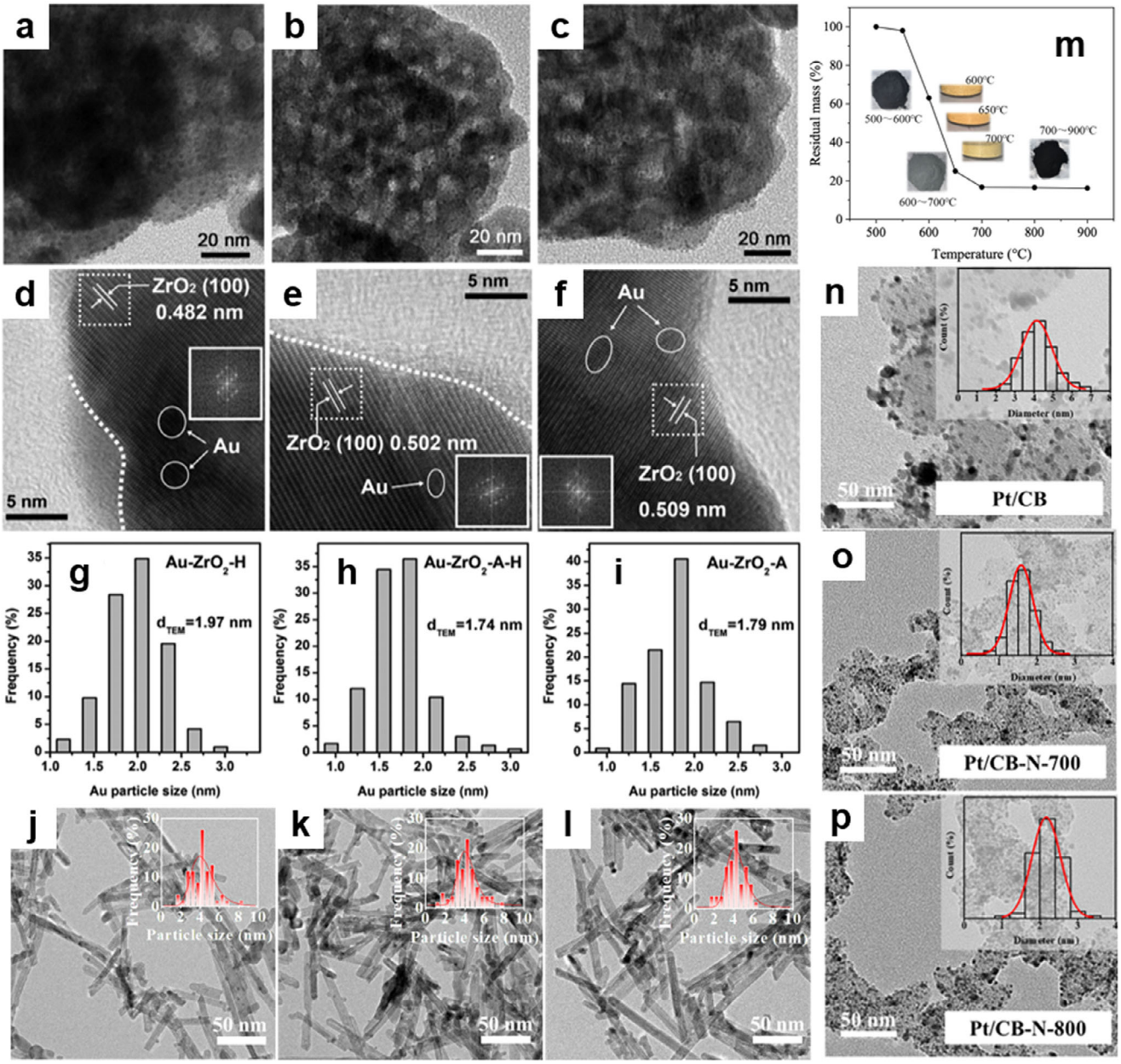

FIGURE 9 | (a–i) TEM images of Au-ZrO_2 catalysts: (a, d)Au-ZrO_2-H; (b, e)Au-ZrO_2-A-H; and (c, f)Au-ZrO_2-A. Distributions of Au cluster diameters (d_{TEM}) in Au-ZrO_2 under different treatment methods [106]. Copyright 2018, American Chemical Society. (j–l) TEM images of X-CeO_2 catalysts: (j)Au/CeO_2; (k)PtAu/CeO_2; l)Pt/CeO_2. [107] Copyright 2024, Elsevier. (m–p) Schematic diagram of the synthesis method of N-doped C support and TEM image and particle size distribution curve of Pt/C [108]. Copyright 2024, American Chemical Society.

hydroxylation), the doping of impurity atoms, and the electronic structure [103–105]. In the preparation of catalysts for the water-gas shift (WGS) reaction, Song et al. used a hydrogen etching method to create oxygen vacancies on the surface of the difficult-to-reduce ZrO_2 as shown in Figure 9a–i, thereby anchoring Au species and successfully preparing an excellent catalyst for the WGS reaction [106]. They proposed that the introduction of surface oxygen vacancies narrows the band gap of ZrO_2 and reduces the ohmic barrier, thereby promoting the flow of "hot electrons." On the other hand, the oxygen vacancies on the ZrO_2 support can easily capture conduction band electrons, and these captured electrons immediately participate in the reduction of H_2O to H_2. Shan et al. also produced excellent WGS low-temperature catalysts by fixing Au clusters on CeO_2. It is worth noting that the average radius of Au clusters on the ZrO_2 surface does not exceed 2 nm, while that on CeO_2 is close to 4 nm (see Figure 9j–l), which fully demonstrates that the role of the support in regulating the size of metal clusters cannot be ignored [107]. These findings highlight that modulating the electronic structure of supports play a decisive role in tuning metal-support charge transfer and stabilizing active metal species. Inspired by this principle, researchers have extended the concept to non-oxide systems, where deliberate electronic modification of carbon-based supports can also optimize catalytic interfaces. Cai et al. found that nitrogen-doping modification of carbon supports can effectively improve the dispersion of Pt nanoparticles, further

enhancing the performance and durability of the catalyst. Their study revealed a positive correlation between the degree of nitrogen doping and the dispersion of Pt, as shown in Figure 9m–p [108]. The average size of Pt nanoparticles was reduced to 1.7–2.5 nm, indicating improved dispersion of Pt. Nitrogen-doped Pt/C catalysts exhibited similar area-specific activity (SA), indicating that nitrogen sites have a limited impact on the intrinsic activity of the catalyst. This suggests that the active nitrogen sites on the carbon support do not contribute significantly to catalytic activity; instead, their influence on particle size and dispersion is the critical factor.

Second, the crystal structure and morphology of the support collectively determine the surface properties of the exposed support, altering the local environment of metal nanoparticles (NPs), thereby regulating NP shape and SMSI. Murata et al. studied the effect of Pd nanoparticle size on methane combustion using alumina supports with different crystalline phases [109]. For Pd/θ-Al_2O_3 and Pd/α-Al_2O_3, which have weak metal-support interactions, catalytic activity showed a volcano-shaped dependence on Pd particle size [110]. Further characterization demonstrated that alumina supports with different crystal phases adjusted the size and morphology of Pd particles, thereby changing the catalytic performance [111, 112]. Other studies have shown that Pd NPs supported on ZnO (100) (higher coordination) and ZnO (001) (lower coordination) facets exhibit markedly distinct sintering behaviors. After calcination at 600°C, Pd particles on the (100) facet demonstrated significant growth from 1.1 to 5.7 nm, whereas those on the (001) facet maintained their original dimensions. This phenomenon rationalizes the divergent catalytic performance trends in CO oxidation between Pd catalysts supported on ZnO (100) and (001), with the latter exhibiting superior activity and stability due to its crystallographic orientation advantages [113]. Wang et al. reported a strategy to reduce the Pt loading to just 0.1 wt%, achieving a stable catalyst with high activity and stability at low temperatures through a silica coating. The interface between the catalyst and the silica coating altered the SMSI to immobilize Ga oxide clusters, further securing the Pt catalytic sites for catalytic reactions. Additionally, the electronic state of Pt was influenced by the silica coating, demonstrating a novel approach to utilizing metal-support interactions in catalysis [114].

Another common method for regulating the support is to modify the surface of the support by introducing other functional groups or coatings to indirectly control the interactions at the interface. Ding et al. employed surface chemical synthesis techniques to introduce intermediates such as tetra ammonium palladium (II) $[Pd(NH_3)_4]^{2+}$ and tetra chloroplatinate $[PtCl_4]^{2-}$, followed by decomposition and reduction of the surface-adsorbed heterometallic double complexes. This approach ultimately enabled the successful preparation of palladium-platinum (Pd-Pt) nanoparticles, which exhibited enhanced catalytic performance in the selective hydrogenation of acetylene [115]. Afterward, Kwak et al. revealed that penta-coordinated Al^{3+} sites on γ-Al_2O_3(100) facets facilitate atomic-level dispersion of Pt species at low loadings [116], where the cation coordinates with five oxygen atoms-three from the alumina lattice. These under-coordinated sites not only permit superior dispersion but also confer enhanced stability. Studies have demonstrated that Pd-based bimetallic nanoparticles synthesized on Al_2O_3 supports with a high abundance of penta-coordinated Al^{3+} sites exhibit reduced mean particle sizes and suppressed sintering compared to conventional Al_2O_3 supports. In related investigations of Ru/γ-Al_2O_3 catalysts, post-thermal treatment during CO_x methanation processes induced increased Lewis basicity at surface hexa-coordinated or penta-coordinated Al sites through OH species formation [117]. This modified surface basicity, combined with enhanced Ru mobility at elevated temperatures, promoted the formation of flattened Ru nanoparticles with improved sintering resistance [118].

Utilizing the reducibility of the supports to regulate SMSI is also a common method. Supports typically exhibit diverse physical and chemical properties, ranging from wide-bandgap insulators to semiconductors, depending on their electronic band structures. These supports are broadly categorized as either "non-reducible" (e.g., Al_2O_3, SiO_2, ZrO_2) or "reducible" (e.g., TiO_2, CeO_2), a classification that fundamentally governs the nature of MSI. The bulk properties of the support can be systematically manipulated through doping or nanostructuring strategies. This allows for a balance between high dispersibility and structural stability in the active AM phase. The strength of the MSI determines the redox properties of the active AM phase and significantly influences its reduction and oxidation behavior at different temperatures during catalyst activation and reaction [119]. As demonstrated in Beale et al.'s study, cobalt NPs supported on SiO_x/Si (100) and rutile TiO_2(110) substrates exhibited markedly distinct reduction profiles and sintering resistance. Co NPs on SiO_x/Si (100) with weaker interactions underwent complete reduction upon H_2 treatment, while their TiO_2 (110)-supported counterparts remained partially reduced under identical conditions. However, the former system showed significant NP migration and agglomeration during reaction, whereas the latter exhibited sufficiently strong interactions to enable Co atom diffusion into the surface and subsurface regions. This principle of engineering-enhanced MSI can be strategically employed to reestablish high dispersion through sequential calcination-reduction treatments, which have proven effective in improving NP dispersion as activation or regeneration protocols [120, 121]. Bruix et al. fabricated model Pt/CeO_2(111) and Pt/CeO_x/TiO_2(110) catalysts, demonstrating maximum water-gas shift (WGS) catalytic activity at a Pt coverage of 0.2 mL [122]. Sub nanometer Pt clusters (θ_{Pt} < 0.25 mL) deposited on oxide supports exhibited depleted d-states near the Fermi level, indicative of substantial Pt→CeO_2 charge transfer inducing significant electronic perturbation. Notably, the 0.2 mL Pt/CeO_x/TiO_2(110) system exhibited such pronounced electronic modulation that complete O-H bond dissociation in adsorbed H_2O occurred, ultimately generating H_2 and O_2. Campbell subsequently formalized the Electronic metal-support interaction (EMSI) concept, emphasizing the adjustment of interfacial chemical bonding and charge transfer at metal-support interfaces to regulate the electronic and catalytic properties of surface sites [123]. It is worth noting that EMSI exhibits pronounced size dependence, as demonstrated by systematic investigation of Pt species on CeO_2 spanning sub nanometer clusters to NPs [124]. Charge transfer from Pt to CeO_2, accompanied by $Ce^{4+} \rightarrow Ce^{3+}$ reduction, reached maximum efficiency in Pt NPs containing 30-70 atoms, corresponding to peak positive charge per Pt atom. This optimal size regime balances two competing factors: smaller Pt clusters exhibit reduced EMSI due to preferential nucleation at pre-existing Ce^{3+} defects, while larger NPs show diminished

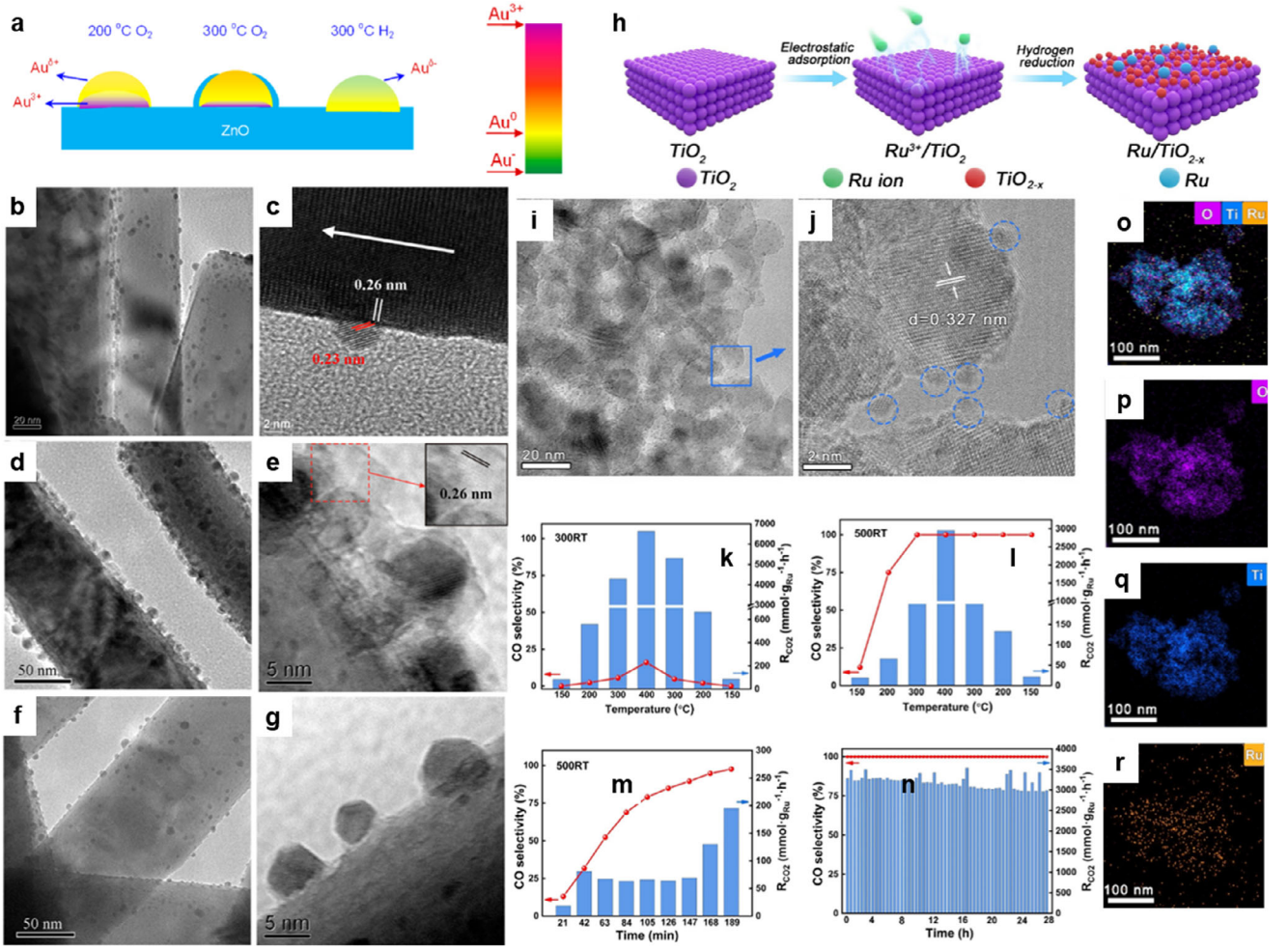

FIGURE 10 | (a–g) Induction of SMSI in the Au/ZnO-nanorod system under an oxidizing atmosphere (b,c) 200°C; (d–e) 300°C, and dynamic disappearance under a reducing atmosphere (f,g) 300°C [127]. Copyright 2012, American Chemical Society. (h) Schematic synthetic procedures for adsorbate-induced SMSI. (i,j) TEM image of A-SMSI. (o–r): elemental mapping images. (k–m) Catalytic performance of (k) without A-SMSI and (l–m) A-SMSI structure. (n) Stability of A-SMSI structure [133]. Copyright 2024, John Wiley and Sons.

charge transfer capacity constrained by surface Ce^{3+} concentration limitations. Theoretical modeling based on metal-support contact principles corroborates this size-dependent EMSI trend, revealing cluster-size governed charge transfer magnitudes: 0.5 e^-/atom for 1.5 nm clusters versus 0.01 e^-/atom for > 10 nm particles [125]. This size-effect paradigm extends to other systems, as evidenced by Ir/CeO_2 catalysts, where CO_2 hydrogenation selectivity transitions from CO to CH_4-selective with increasing particle size. Parallel observations in Ru/TiO_2 systems further validate the universality of EMSI-mediated size-dependent catalytic modulation [126].

3.3 | Pretreatment Conditions

High-temperature reduction treatment is the most common method for modulating SMSI, which is attributed to the generation of metal cations and oxygen vacancies. Recently, high-temperature oxidation treatment has also been identified as an effective approach for regulating SMSI. Liu et al. were the first to successfully construct SMSI under high-temperature oxidation conditions in Au-supported ZnO nanorods, defining it as oxidative SMSI (O-SMSI), as shown in Figure 10a–g [127]. Subsequently, other researchers also successfully achieved O-SMSI in Au/TiO_2 and Pt/TiO_2 systems using melamine and nitrogen. The encapsulation layer formed by this O-SMSI is exceptionally stable under oxidative conditions [128–130]. The formation mechanism of this phenomenon remains unclear, but the prevailing hypothesis suggests that under low oxygen partial pressure, lattice oxygen atoms can migrate at high temperatures, forming metal-O-metal interfacial bonds, thereby achieving high stability in oxidative environments [131, 132]. In addition, some researchers have found that the high coverage adsorption of specific reaction intermediates on the support surface can induce the formation of oxygen vacancies. These intermediates subsequently migrate from the support to the metal, leading to the formation of an encapsulation structure. This adsorbate-induced SMSI is referred to as A-SMSI [133, 134]. The A-SMSI encapsulation layer exhibits unique chemical properties; the SMSI effect induced by temperature-regulated adsorbates enables the catalyst to exhibit excellent activity and stability in the reverse water-gas shift reaction, which is attributed to the presence of HCO_x within the encapsulation layer, as shown in Figure 10h–r. For inert MgO and Au

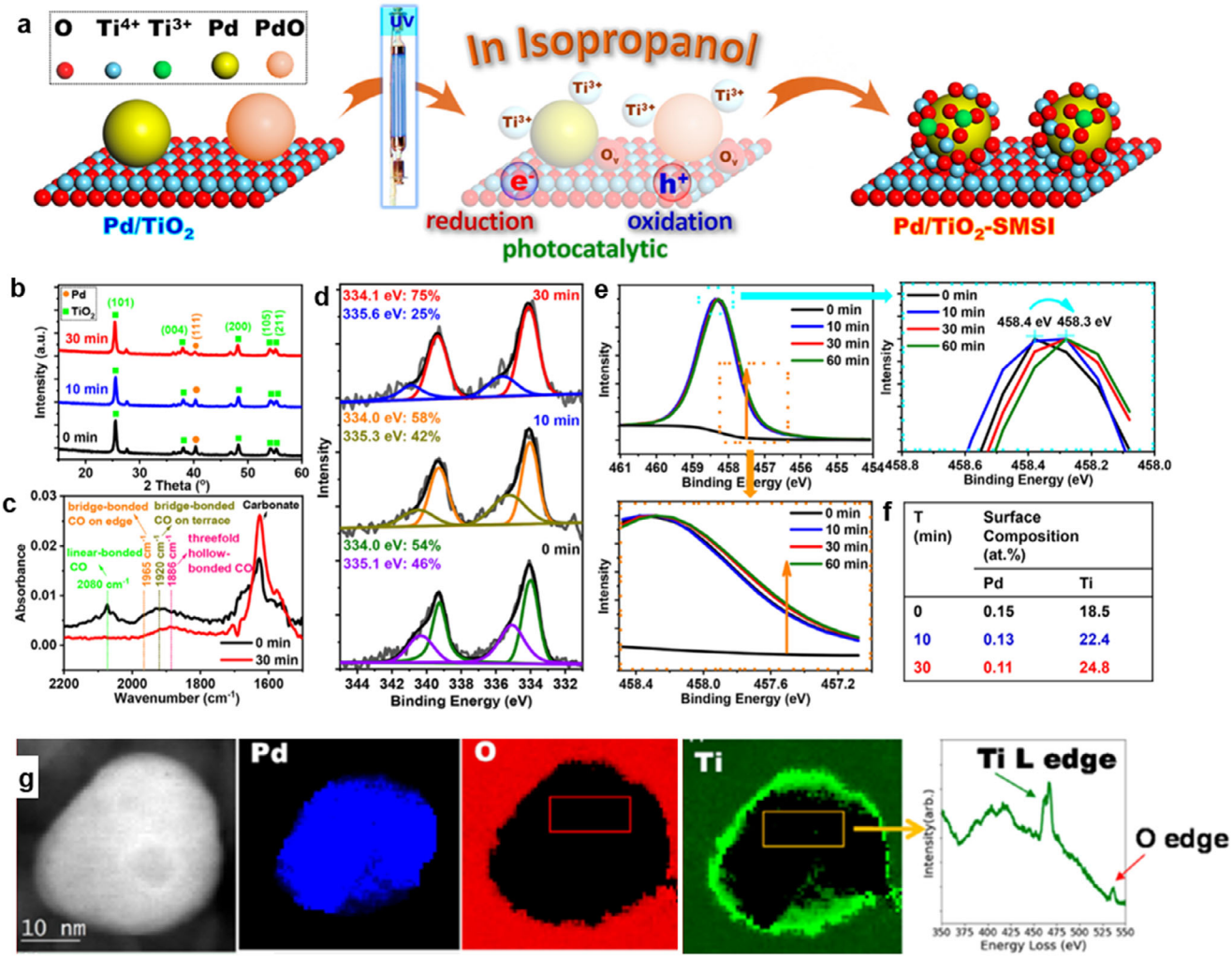

FIGURE 11 | (a) Schematic illustration of photochemistry-promoted Pd/TiO_2-SMSI construction. (b–f) Characterizations of the Pd/TiO_2 precursor and Pd/TiO_2-SMSI-t (t = UV irradiation time). (b) PXRD patterns; (c) CO-DRIFTS spectra; (d) Pd 3d XPS spectra; (e) Ti 2p XPS spectra; (f) surface composition from XPS. (g) STEM-ADF images, EELS maps, and Ti L-edge EELS spectra from orange box regions for Pd/TiO_2-SMSI-30 min [137]. Copyright 2021, American Chemical Society.

nanoclusters, Wang et al. successfully constructed SMSI under a flowing CO_2 atmosphere. The acidic CO_2 activated the basic MgO support, leading to the formation of carbonates, which decomposed at appropriate temperatures [135]. Interestingly, the dynamically formed MgO exhibited significantly higher mobility than the original MgO support, facilitating the formation of the encapsulation layer. The team validated their hypothesis of dynamic evolution using Au clusters directly supported on $MgCO_3$ [136]. In addition to various gas atmospheres, Zhang et al. achieved SMSI construction at room temperature through redox interactions between $Au^{\delta+}$ and Ti^{3+} precursors, successfully enhancing CO conversion rates. This approach has the advantage of avoiding nanoparticle sintering at high temperatures [86]. Chen et al. discovered that ultraviolet (UV) irradiation can also regulate SMSI. For TiO_2 semiconductor supports, when the energy provided by UV light exceeds its bandgap, separated reductive electrons (e^-) and oxidative holes (h^+) are generated, thereby triggering the formation of Ti^{3+} and oxygen vacancies, as shown in Figure 11a. [137] The characterization images in Figure 11b–g also confirm that the UV-irradiated TiO_2 forms a TiO_x capping layer with abundant Ti^{3+} species and Ov in the framework. Similarly, ultrafast lasers have been employed to construct SMSI in Pt/CeO_2 systems. The laser facilitates the formation of localized electric fields at the Pt NPs-CeO_2 interface, promoting the generation of surface oxygen vacancies and the migration of metastable CeO_x, as shown in Figure 12a–g [138]. The formation of laser-induced SMSI markedly enhanced the catalyst's performance during CO oxidation, improving both its activity and stability. The encapsulation layer remained intact after reaction, demonstrating high stability. This photochemical approach can even be extended to non-reducible oxide supports, such as Al_2O_3 and MgO [139]. Wang et al. also used a high-temperature treatment method to dynamically convert Mg and Al hydroxides into oxides to achieve SMSI, obtaining a thermodynamically stable structure under reaction conditions [140]. As novel experimental methods are gradually discovered, the original framework and limitations of SMSI (such as dependence on high temperature and reducing atmosphere) are slowly being broken, allowing us to achieve the regulation of SMSI under more general reaction conditions. Therefore, continuing to develop new methods to induce SMSI is of important and far-reaching significance.

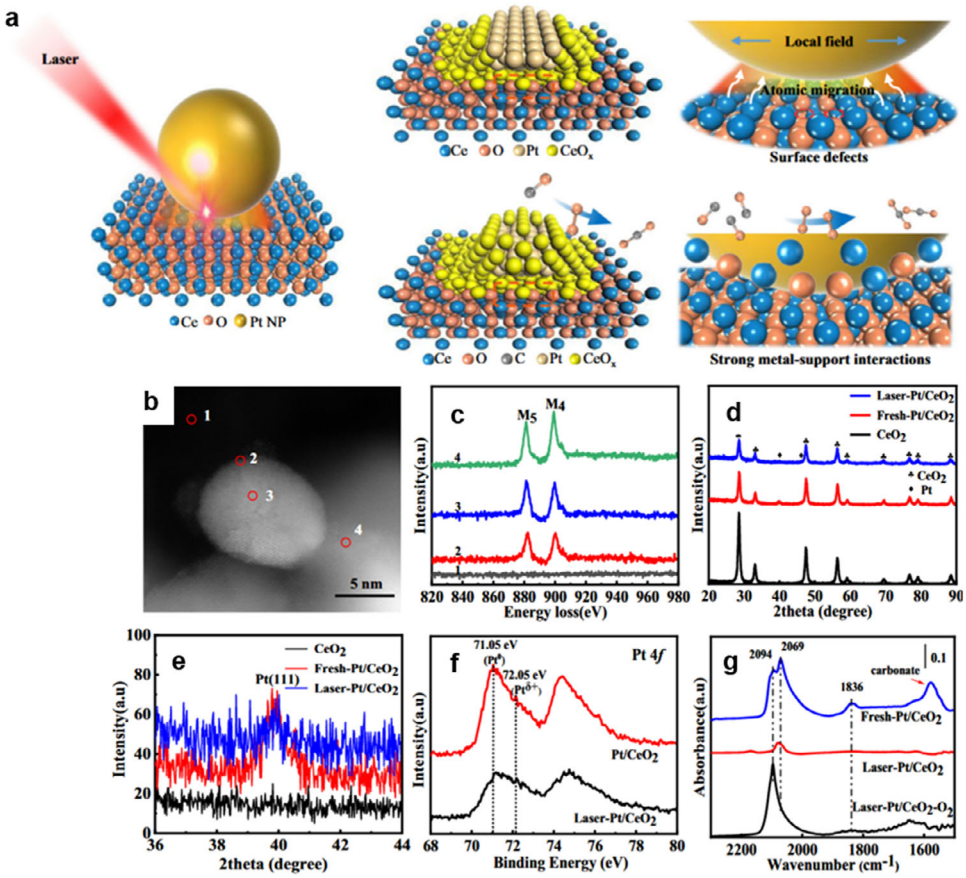

FIGURE 12 | (a) Schematic of the ultrafast laser-induced SMSI in Pt/CeO_2. (b) High-angle annular dark-field scanning transmission electron microscopy (HAADF-STEM) image of laser-irradiated Pt/CeO_2. (c) EELS spectrum of laser-irradiated Pt/CeO_2. (d, e) XRD spectra of Pt/CeO_2 and laser-irradiated Pt/CeO_2. (f) XPS spectra of fresh Pt/CeO_2 and laser-irradiated Pt/CeO_2. (g) In situ CO-DRIFT of fresh Pt/CeO_2 and laser-irradiated Pt/CeO_2 [138]. Copyright 2021, Springer Nature.

3.4 | Application of SMSI in Heterogeneous Catalysis

The surface chemisorption properties of catalysts exert a profound influence on their catalytic performance. This phenomenon becomes particularly pronounced in catalysts exhibiting strong interaction, where the strong chemical bonds formed at the interface can substantially modify the chemisorption behavior of supported metals. Water electrolysis poses significant challenges to the catalytic activity and stability of oxygen evolution reaction (OER) electrocatalysts. Rational support design plays a pivotal role in polymetallic oxide systems, where optimizing the interplay among conductivity, catalytic activity, and stability is of paramount importance. To address this challenge, Wang et al. engineered an asymmetric redox chemistry by constructing a defect-rich Ni/Fe LDH nanosheet with single-atom Ru modification, featuring surface OO-Ru-OH and bulk-phase Ru-O-Ni/Fe coordination, which is coupled with SMSI [25]. Spectroscopic characterization and theoretical calculations revealed that single-atom Ru can redistribute the O 2p electrons on the surface and optimize the d-electron configuration of metal atoms in the bulk phase through SMSI. The enhanced surface lattice oxygen, stabilized bulk lattice oxygen, and stronger adsorption of oxygen-containing intermediates by the bulk metal were confirmed by ^{18}O isotope labeling experiments, chemical probe experiments, and theoretical calculations. Kim et al. developed a rational synthesis strategy for constructing active site/oxide support junctions in OER electrocatalysts, with particular emphasis on achieving the critical balance among activity, stability, and conductivity (Figure 13a–c). The researchers leveraged catalyst-support interactions to enhance both the intrinsic activity and durability of Ir-based catalysts. While Mo doping energetically facilitated the formation of high-valent Ir species and thereby improved intrinsic catalytic activity, it concurrently resulted in reduced electrical conductivity. The results demonstrate that the interfacial structures formed by metal oxide supports play a pivotal role in enhancing the stability of Ir catalysts, as evidenced by comparable ASF values between supported catalysts and bulk IrO_x, as shown in Figure 13d–g. In situ stability analysis combined with IL-STEM revealed the complex, potentially dependent behaviors of different support materials, highlighting the necessity of evaluating catalyst and support dissolution as an integrated system [141].

Beyond regulating catalyst stability, researchers have also attempted to utilize the encapsulation structures formed through SMSI to achieve favorable electronic configurations that facilitate catalytic reactions. Wang et al. applied the concept of regulating SMSI to fabricate Ru/TiN catalysts with varying degrees of TiN coverage on Ru nanoparticles, and applied them to alkaline water electrolysis, as shown in Figure 13h [142]. Characterization revealed that, as the SMSI degree increased, the TiN coverage

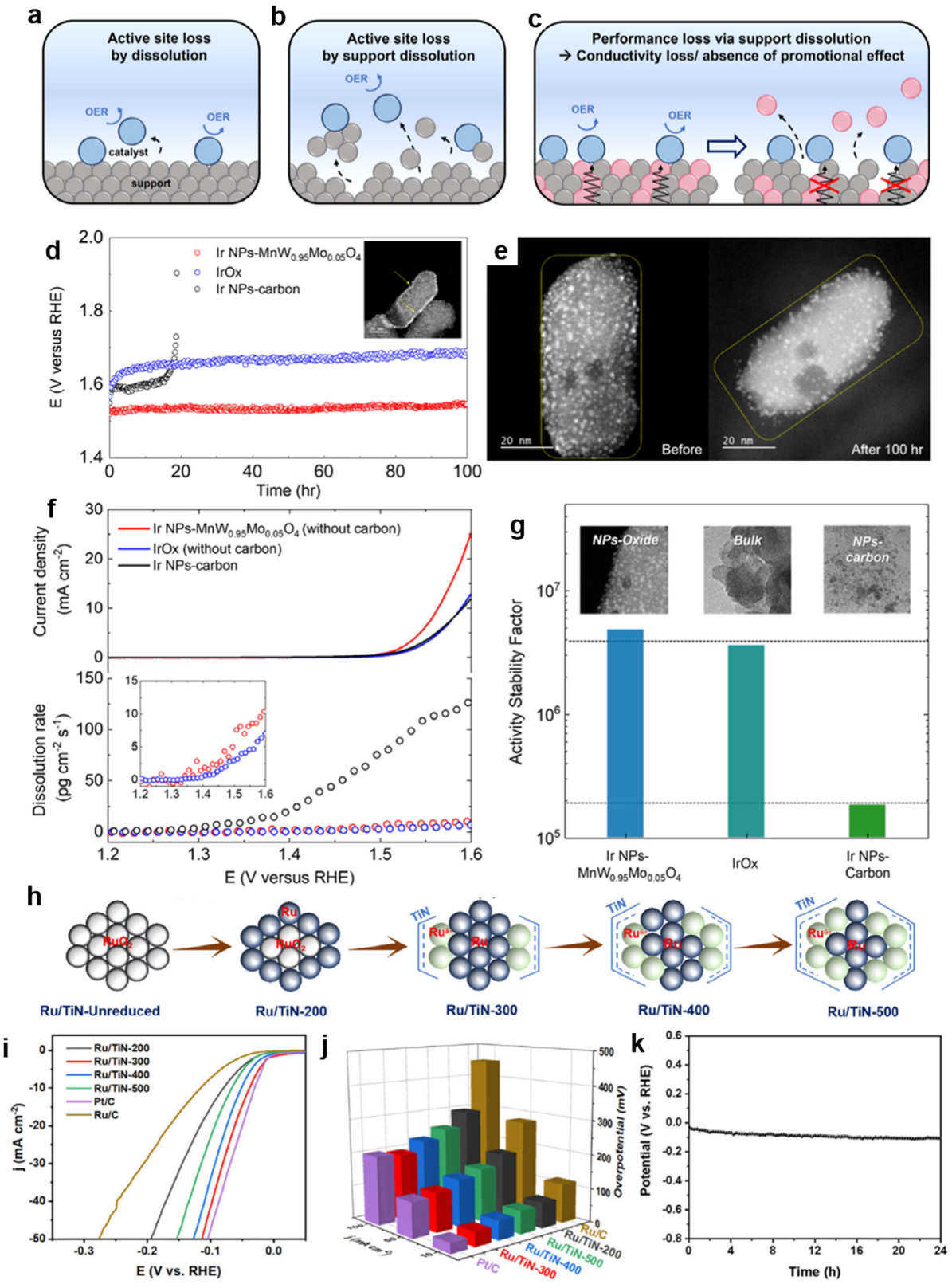

FIGURE 13 | (a–c) Conceptual schematics illustrating different degradation pathways via elemental dissolution. (d) Chrono potentiometric stability test. (e) HAADF-STEM images of Ir NPs on $MnW_{0.95}Mo_{0.05}O_4$ before and after OER operation. (f) Linear sweep voltammetry (LSV) curves (top) and in situ ICP-MS-derived Ir dissolution rates (bottom) under OER conditions. (g) Comparison of the activity stability factor (ASF) across different catalysts [141]. Copyright 2025, American Chemical Society. (h) A schematic illustration of the structural evolution of Ru/TiN at different stages of reduction. (i) HER polarization curves, and (j) overpotentials for various catalysts. (k) Long-term durability test for Ru/TiN-300 [142]. Copyright 2023, John Wiley and Sons.

progressively encapsulated the Ru nanoparticles, and the Ru-N-Ti bonds induced more electrons to transfer from the Ru nanoparticles to the TiN support. Further studies showed that the exposed Ru-TiN interface significantly enhanced the hydrogen desorption (H_2 dissociation) capability. As a result, Figure 13i–k shows the Ru/TiN with moderate SMSI exhibited excellent hydrogen evolution reaction (HER) performance and stability.

Certain complex chemical reactions with multiple reactants often require multiple active sites and are typically challenging to achieve high conversion rates and selectivity. As illustrated in Figure 14a, depicting the schematic of dry methane reforming, the multi-gas reaction system demands increased adsorption sites, presenting a significant technical challenge for catalyst structural design. SMSI plays an important role in heterogeneous catalysis by partially restructuring supported metal catalysts [143]. Qiao et al. demonstrated that an operando CO_2 induced SMSI (CO_2-SMSI) appears in a single Rh atom doped CeO_2-based materials, significantly enhancing the catalytic activity of the DRM reaction, as shown in Figure 14b,e,f [144]. The formation of appropriate Rh/Rh species is crucial for improving C-H bonds activation, and the presence of a permeable encapsulating layer helps provide more active sites (Figure 14c,d). This discovery offers a new approach to overcoming the limitations of classical SMSI catalysts in DRM reactions. Conventional understanding held that the encapsulation effect of supports on metal NP catalysts occurred almost exclusively with active oxide supports, typically blocking surface catalytic reactions [127, 145]. However, this classical SMSI phenomenon was surprisingly observed between metal NPs (e.g., Ni, Fe, Co, and Ru) and inert hexagonal boron nitride (h-BN) nanosheets. In their study of DRM, Bao et al. utilized weakly oxidizing gases like CO_2 and H_2O to induce the formation of an inert ultrathin boron oxide (BO_x) overlayer encapsulating Ni NPs on h-BN supports (denoted as Ni@BO_x/h-BN). Remarkably, the surface B–O and B–OH sites in the resulting BO_x encapsulation layer cooperated synergistically with surface Ni sites to promote rather than inhibit the DRM process (Figure 14g,h) [24]. This discovery provides new insights for designing novel SMSI-based heterogeneous catalysts.

For catalytic systems where partial encapsulation structures hinder reaction performance, modulating SMSI to control encapsulation formation or dynamically remove such structures has become a key research focus in heterogeneous catalysis. For instance, surface-adsorbed Rh single atoms tend to become encapsulated by ZrO_2 supports after calcination in air, but can be re-exposed through H_2 reduction (see Figure 15a). Wang et al. demonstrated that oxidizing SMSI-generated embedded Rh species created structures with enhanced stability compared to conventional adsorbed configurations, as shown in Figure 15b–d [147]. Figure 15e–i addressed the sintering issue of conventional copper-based catalysts in reverse water-gas shift (RWGS) reactions at high temperatures by modulating SMSI formation through doping Cu NPs with various metals (e.g., Mg, Al, Zn, Zr) [148]. Under high-temperature reaction conditions, excessive SMSI can cause the metal particles to be covered by the support, resulting in a reduction in active sites and hindering the contact between reactants and active sites, thus affecting the catalytic activity. For example, Zn doping significantly suppressed the formation of SMSIin TiO_2, reducing the reducibility of TiO_2 and suppressing the electron transfer between the substrate and metal clusters [148].

4 | In Situ Characterization and Theoretical Modeling Techniques for SMSI

Extensive researchers confirmed that SMSIs can play a pivotal role in significantly enhancing catalytic performance and selectivity under certain conditions in recent decades. A fundamental understanding of SMSI effects on catalytic properties is crucial for the rational design and optimization of high-efficiency catalysts. To gain in-depth understanding of the chemical nature of SMSIs and their mechanistic roles in catalytic reactions, researchers have developed advanced in situ/operando characterization techniques and theoretical modeling techniques, especially machine learning (as presented in Figure 16)[149, 150]. These approaches provided powerful tools for elucidating the chemical essence of SMSIs and their underlying catalytic mechanisms [151–153].

4.1 | Electron Microscopy and X-Ray Spectroscopy

Modern electron microscopy techniques allow us to clearly observe the oxide layer encapsulating the surface of metal nanoparticles. However, when the concept of SMSI was first proposed in the 1970s, electron microscopy could only be used to observe the particle size of metal nanoparticles. With the development of electron microscopy techniques, by the 1980s, Singh et al. were the first to observe, through electron microscopy, that after high-temperature reduction treatment, the Rh nanoparticles in Rh/TiO_2 catalytic materials were encapsulated by an amorphous thin oxide layer (TiO_x) [159]. Subsequently, Logan et al. and Braunschweig et al. further discovered that under high-temperature reduction-oxidation conditions, the encapsulation layer on the surface of Rh nanoparticles in Rh/TiO_2 could be freely rebuilt and peeled off. This discovery provided important clues for understanding the formation mechanism of the encapsulation layer [160]. With the continuous refinement of microscopy, high-resolution transmission electron microscopy (HRTEM) and aberration-corrected TEM have emerged, offering sub-angstrom resolution capable of resolving individual atoms. These advances allowed unprecedented insights into atomic-scale structures, such as lattice fringes, metal-support interfaces, and defect sites. Furthermore, researchers can not only use electron microscopes to observe the encapsulation structure in the SMSI system, but also combine electron energy loss spectroscopy (EELS) and energy dispersive X-ray spectroscopy (EDX) with TEM to simultaneously analyze elemental composition and electronic states, greatly expanding the scope of research on the fine structure of SMSI. For instance, in the Cu/ZnO system, aberration-corrected HRTEM and HAADF-STEM characterization revealed numerous bulk/surface defects in Cu NPs, such as stacking faults leading to the formation of twin boundaries, kinks, and step sites. These observations confirmed the existence of strong interactions between the Cu NPs and ZnO support [161]. Furthermore, electron microscopy demonstrated the migration of disordered ZnO_x overlayers onto Cu NPs, forming encapsulation structures. Additionally, the presence of positively charged $Zn^{\delta+}$ species at the interface was identified through Zn-$L_3M_{45}M_{45}$

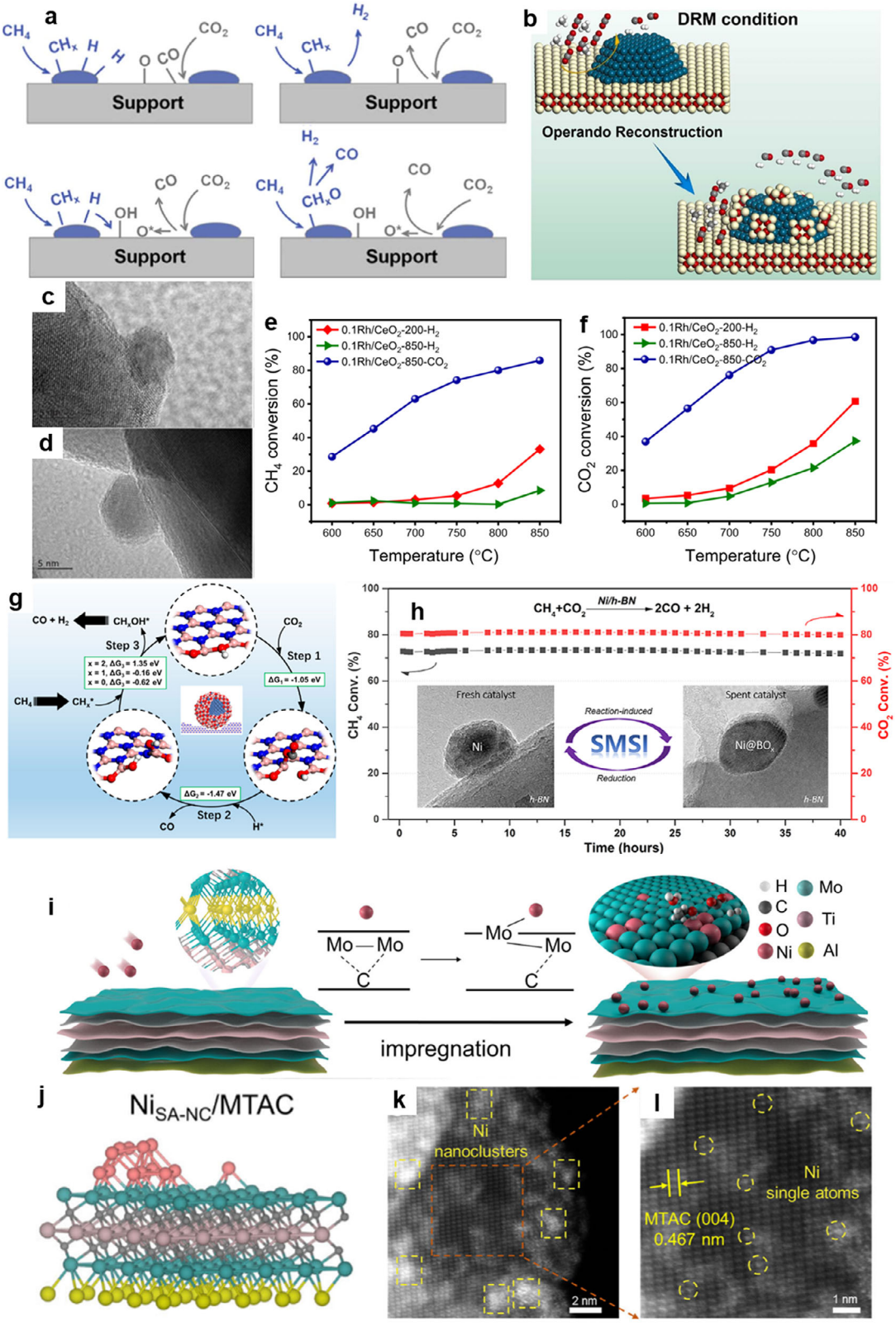

FIGURE 14 | (a) Schematic diagram of methane dry reforming reaction. (b) Schematic diagram of CO_2-SMSI. (c, d) HRTEM images of Rh/CeO_2-850-CO_2 after methane dry reforming reaction. (e, f) Catalytic performance of H_2-treated and CO_2-treated Rh/CeO_2 catalysts in DRM reaction at different reaction temperatures. [144] Copyright 2024, Elsevier. (g) DRM catalytic cycle on Ni@BO_x based on experimental and DFT calculation results. (h) The promotion effect of SMSI encapsulation structure formed on inert oxide BO_x support on DRM reaction [24]. Copyright 2020, American Chemical Society. (i) Schematic illustration of the SRE with applied as prepared Ni/MTAC catalysts for renewable hydrogen production. (j) Structures over Ni_{SA-NC}/MTAC. (k, l) Magnified HAADF-STEM images of 1Ni/MTAC [146]. Copyright 2025, Springer Nature.

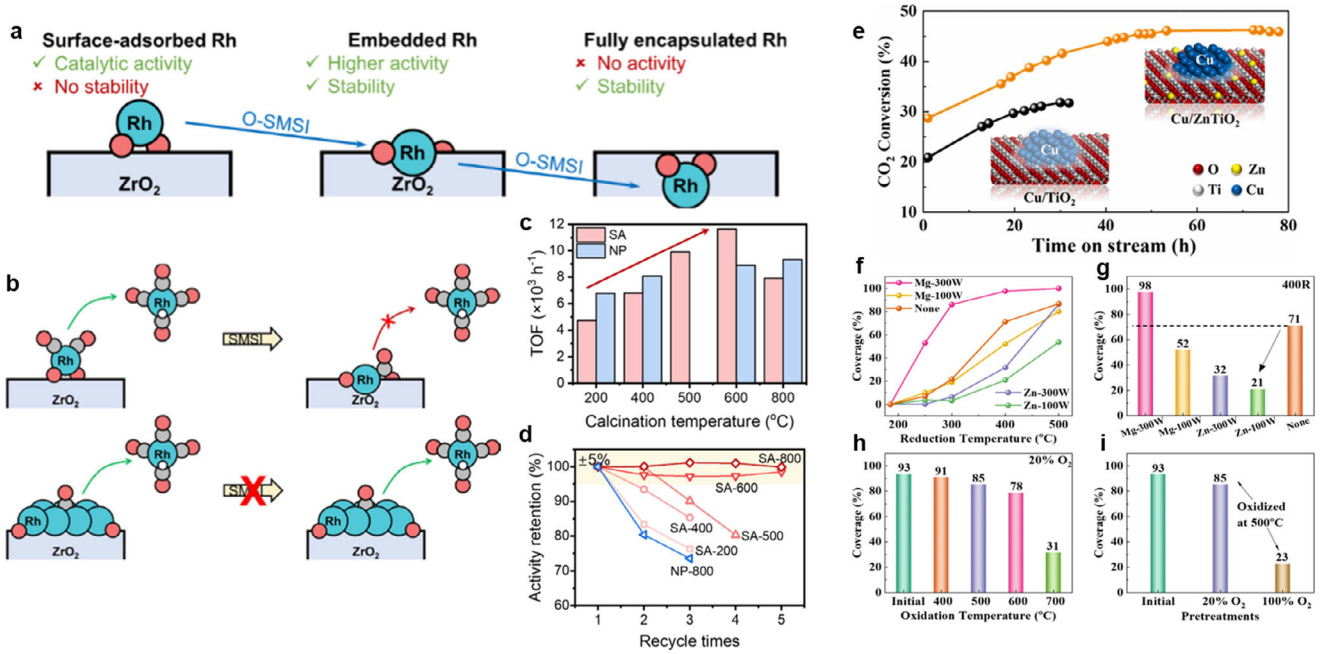

FIGURE 15 | (a) Schematic diagram of Rh SACs during O-SMSI Process. (b) Schematic diagram illustrating the stability enhancement of the O-SMSI on Rh single atoms. (c, d) Comparison of catalytic activity and stability of Rh_1/ZrO_2 and Rh_n/ZrO_2 catalysts [147]. Copyright 2025, American Chemical Society. (e) Structure schematic diagram of $Cu/ZnTiO_2$. Effect of sputtering power and oxidation treatments. (f) Coverage of $Cu/MgTiO_2$ and $Cu/ZnTiO_2$-5 prepared by the SP method compared with the Cu/TiO_2 catalyst without dopants. (g) Comparison of coverage for different Cu-based catalysts that reduced at 400°C. (h) Coverage of $Cu/ZrTiO_2$ after 20% O_2/Ar pretreatments at different temperatures. (i) Coverage of $Cu/ZrTiO_2$ after pretreatment with different oxygen concentrations at 500°C [148]. Copyright 2023, Elsevier.

Auger spectroscopy, indicating the occurrence of SMSI between Cu and ZnO [162].

While electron microscopy has laid the foundation for researchers' understanding of the structure-function integration of catalysts, traditional electron microscopy techniques are limited to ex-situ observation, typically providing only static snapshots of synthesized or reacted materials. Since SMSI exhibits dynamic structural changes under reaction conditions, in situ and operando characterization techniques are needed to address this challenge and bridge the gap between ideal model systems and industrially relevant catalyst systems.

Understanding the dynamic evolution processes of catalysts has drawn researchers' attention to potential active sites. Over the past decades, extensive studies using in situ or operando characterization techniques have been conducted on the structures of metal nanoparticles (such as Au, Pt, Cu, and Ni), revealing the dynamic evolution processes of catalysts and their impacts on catalytic reactions [163–166]. Generally, dynamic behaviors include surface reconstruction, size variation, phase transitions, and compositional changes. Among these studies, in situ microscopy techniques play a crucial role in dynamic catalysis as they directly visualize the temporal changes in catalysts. For instance, Hansen et al. were the first to achieve atomic-resolution visualization of the dynamic structural changes in supported Cu nanoparticles under reaction conditions using environmental transmission electron microscopy (ETEM) [167]. Their work revealed that nanoparticles undergo dynamic shape changes during reactions. Later, Hakeda et al. also used ETEM to observe the dynamic behavior of CeO_2-supported Au (100) in the presence of adsorbed CO molecules at room temperature [168]. Their experiments demonstrated that the Au surface reconstructs itself based on the surrounding gas environment. Additionally, Wang and colleagues utilized in situ ETEM to observe the dynamic transformations of Au nanoparticles [169]. They discovered that under working conditions, larger gold nanoparticles remained rigid, while ultrasmall clusters transformed into a liquid-like disordered structures. These size-dependent dynamic changes are crucial for enhancing activity and selectivity, thus underscoring the significance of in situ techniques in designing high-performance catalysts. Previous studies observed surface melting of gold nanoparticles (2–5 nm in diameter) supported on carbon films as the temperature increased, using in situ heating stages in aberration-corrected scanning transmission electron microscopy (ac-STEM) [170]. At 25°C, the structure of gold nanoparticles underwent dynamic transitions, forming a solid core-liquid shell structure.

In addition to microscopy characterization methods, in situ or operando spectroscopic techniques, such as X-ray Photoelectron Spectroscopy (XPS), X-ray Absorption Spectroscopy (XAS), and Extended X-ray Absorption Fine Structure (EXAFS), have been successfully applied to track the dynamic behavior of catalysts under reaction conditions. Unlike microscopy techniques, these spectroscopic methods can reveal the electronic structure, oxidation state, and coordination environment of the active sites during the SMSI process. This helps researchers gain a better understanding of the real-time changes in both the structure and activity of the catalyst throughout the reaction. For example, Pu et al. observed a dramatic and reversible reconstruction of Ce^{3+} sites because of SMSI by using in situ XPS [171]. A single

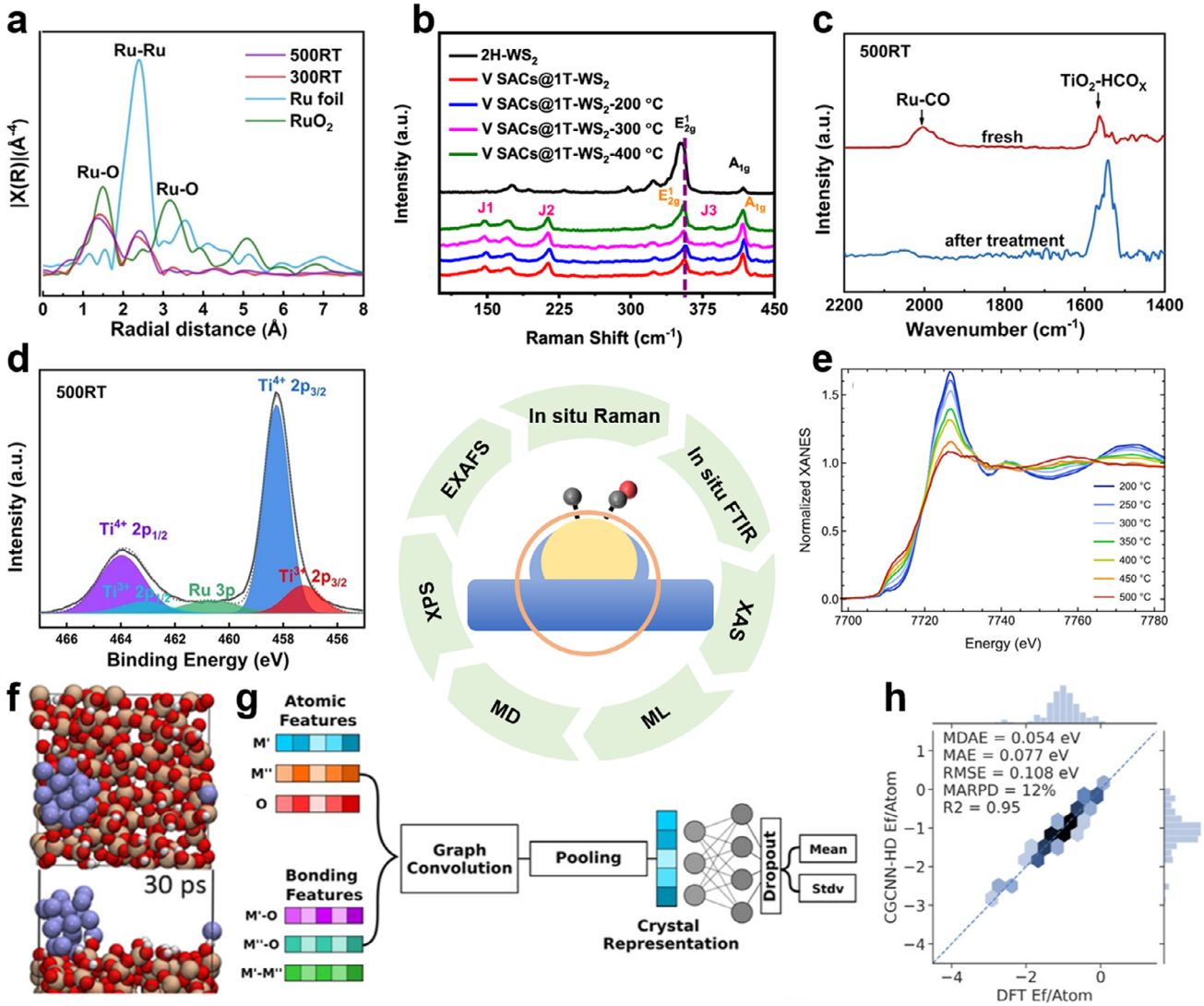

FIGURE 16 | Overview of techniques applied in characterization of SMSI phenomena. (a) EXAFS results of RuO_2. [133] Copyright 2024, John Wiley and Sons. (b) Raman spectroscopy [154]. Copyright 2021, Springer Nature. (c) DRIFTS [155] Copyright 2025, American Chemical Society. (d) X-ray photoelectron spectroscopy of Ru/TiO_2 [133]. Copyright 2024, John Wiley and Sons. (e) XAS plots of Co_2Pt_3 [156]. Copyright 2021, American Chemical Society. (f) Advanced ab initio molecular dynamics simulations of Ag/Al_2O_3 [157]. Copyright 2025, American Chemical Society. (g) CGCNN-HD model architecture. (h) Parity plot of RuO_2 samples [158]. Copyright 2024, American Chemical Society.

characterization method is often limited, and it is difficult to fully understand the dynamic process of catalytic reactions. In order to explore the complete dynamic behavior, it is usually necessary to integrate multiple operando techniques to capture multiple perspectives on structure and electronic properties. Liu et al. systematically studied the dynamic evolution of the Pt clusters structure in the water-gas shift reactionunder the influence of SMSI from different supports through a complete characterization methods [172–175]. They also confirmed that the CO oxidation reaction is closely related to the size and electronic structure of the Pt clusters, and further extended this conclusion to the Pt-Sn clusters [176–178]. These studies demonstrate the important role of advanced characterization techniques in studying the dynamic behavior of SMSI.

Recent advances in in situ and operando characterization techniques have greatly deepened our understanding of SMSI, unveiling the dynamic evolution of metal-support interfaces under reaction conditions. The continuous improvement of synchrotron-based spectroscopy, environmental TEM (ETEM), and near-ambient pressure XPS (NAP-XPS) now enables real-time visualization of interfacial dynamics under realistic environments, allowing a shift from static observation to mechanistic insights. The integration of multimodal approaches, including in situ TEM, XAS, and vibrational spectroscopy, further enhances the ability to correlate atomic-scale structures with electronic properties and catalytic performance.

Nevertheless, significant challenges remain. Capturing atomic-level processes under realistic high-temperature and high-pressure conditions is still difficult, and current experimental configurations often deviate from true catalytic environments. Moreover, the transient and multiscale nature of SMSI, coupled with the interplay of electronic, geometric, and interfacial

migration effects, complicates quantitative interpretation. Future advances will rely on developing operando-compatible systems with higher spatial and temporal resolution, combining multimodal data fusion with intelligent analysis, and integrating experimental observations with theoretical modeling. In particular, density functional theory (DFT) and molecular dynamics (MD) simulations serve as indispensable complements, providing atomistic insights into the energetics, charge transfer, and interfacial reconstruction mechanisms that govern SMSI phenomena.

4.2 | Theoretical Computational Research

The development of theoretical computational science is of great significance for exploring the impact of SMSI on the interfacial properties of catalytic materials. Various computational methods are widely applied to theoretical studies of SMSI systems at different scales, such as Density Functional Theory (DFT), Ab initio molecular dynamics (AIMD). Although substantial research on SMSI has been conducted over the past few decades, the SMSI process remains complex and challenging to fully understand due to the involvement of multiple intricate interactions [179, 180]. However, with advancements in computational technology and theoretical chemistry methods, techniques such as DFT have emerged as powerful tools for elucidating reaction mechanisms. These methods provide additional insights and critical information that can guide the design of high-performance catalysts. Recently, computational chemistry has become an integral part of catalytic research. By predicting descriptors associated with catalytic activity, such as adsorption energy, activation energy, and the d-band center, researchers can significantly enhance their understanding of the atomic-level mechanisms underlying heterogeneous catalytic processes. This approach enables the rational design of catalysts with improved efficiency and selectivity, driving innovation in the field. DFT has been effectively employed to provide complementary insights into various catalytic phenomena at the electronic level, shedding light on reaction mechanisms and processes. Wang et al. investigated the influence of the dynamic structural evolution of $Cu_4/CeO_2(110)$ under water-gas shift reaction (WGSR) temperatures on its catalytic activity. DFT calculations revealed that the charge variations induced by oxygen vacancy formation at different reaction temperatures significantly affect the adsorption energies of reaction intermediates, as illustrated in Figure 17a–c. These charge variations simultaneously modulate the interaction strength between the cluster and the interface.Concurrently, they used microkinetics to further reveal the adsorption activity and reaction rates of intermediate species at different temperatures, as shown in Figure 17d–f, providing theoretical guidance for setting the conditions for catalytic reactions. Leveraging this SMSI regulation mechanism, the researchers successfully designed an optimized catalyst system for the WGSR [181]. Mohan and colleagues utilized DFT and microkinetic modeling to study the dry reforming of methane (DRM) reaction network on nickel-based catalysts. Their work elucidated the primary reaction pathways of fundamental processes and the mechanisms leading to the formation of final and side products. Additionally, they explored the influence of SMSI on the C—H bond dissociation mechanism, offering a deeper understanding of the reaction steps [182].

Moreover, given the tendency of oxides to readily form oxygen vacancies and the challenges in quantitatively characterizing them experimentally, DFT calculations are frequently used to compute surface chemistry Pourbaix diagrams [185]. These diagrams help predict the thermodynamic stability of various surface states under different environmental conditions, providing critical insights into the design of robust catalysts with tailored properties, as shown in Figure 17g [183, 186, 187]. This combination of DFT and theoretical modeling significantly enhances the understanding of complex catalytic systems and SMSI-related phenomena. In the study of the Pd/TiO_2 system, Zheng et al. demonstrated that the oxygen-vacant TiO_2 can concurrently downshift the d-band center of Pd and facilitate hydrogen spillover, thereby accelerating H desorption and FOR kinetics [184]. The results in Figure 17h–l show the electronic structure before and after defect formation. The differences in work function and d-band center correspond to the changes in the potential catalytic activity, while the differential charge diagram and COHP diagram illustrate the binding strength of Pd clusters to TiO_2. Fan and colleagues, through studies on interfacial structures, catalytic activity, and atom-level DFT calculations, revealed that the SMSI effect at the copper-silica interface promotes activity in transfer hydrogenation reactions [188]. Their research highlighted the synergistic interaction between copper clusters and atomic copper species. These sub-nanometer composite materials can be derived from simple synthesis strategies leveraging the SMSI effect in metal-inert support systems. Furthermore, the real active sites of copper-based catalysts were accurately identified, paving the way for the broader application of sub-nanometer materials in industrial catalysis.

DFT calculation methods can easily and accurately obtain information such as the electronic structure properties and reaction energy barriers of the system. Like experimental characterization techniques, other types of calculational methods are needed to complement DFT methods to obtain information about the dynamic behavior of reactions. The advancement of in-situ experimental techniques has opened new avenues for researchers to investigate the dynamic structural evolution of catalysts [189, 190]. In parallel, theoretical computations have made significant contributions to understanding dynamic catalytic mechanisms. Small metal clusters, due to their multiple energy minima, undergo dynamic transitions among energetically similar isomers under high-temperature conditions. This structural flux enhances the catalyst's adaptability but also adds complexity to its behavior. Efforts have been made to identify as many isomeric structures as possible using global optimization methods. However, the limited sampling capacity of such methods often hinders a comprehensive description of complex dynamic catalytic processes. Molecular dynamics (MD) simulations address this limitation by enabling extensive configuration sampling, providing statistical insights into dynamic catalytic mechanisms. Classical MD typically relies on predefined empirical potentials. However, due to their overly simplified descriptions of atomic interactions, no universal empirical force field can accurately represent the formation and breaking of various chemical bonds. Consequently, classical MD is unsuitable for molecular simulations of catalytic reactions. In contrast, AIMD evaluates interatomic forces through precise electronic structure calculations [191, 192]. This enables the study of chemical processes while accounting for the contributions of

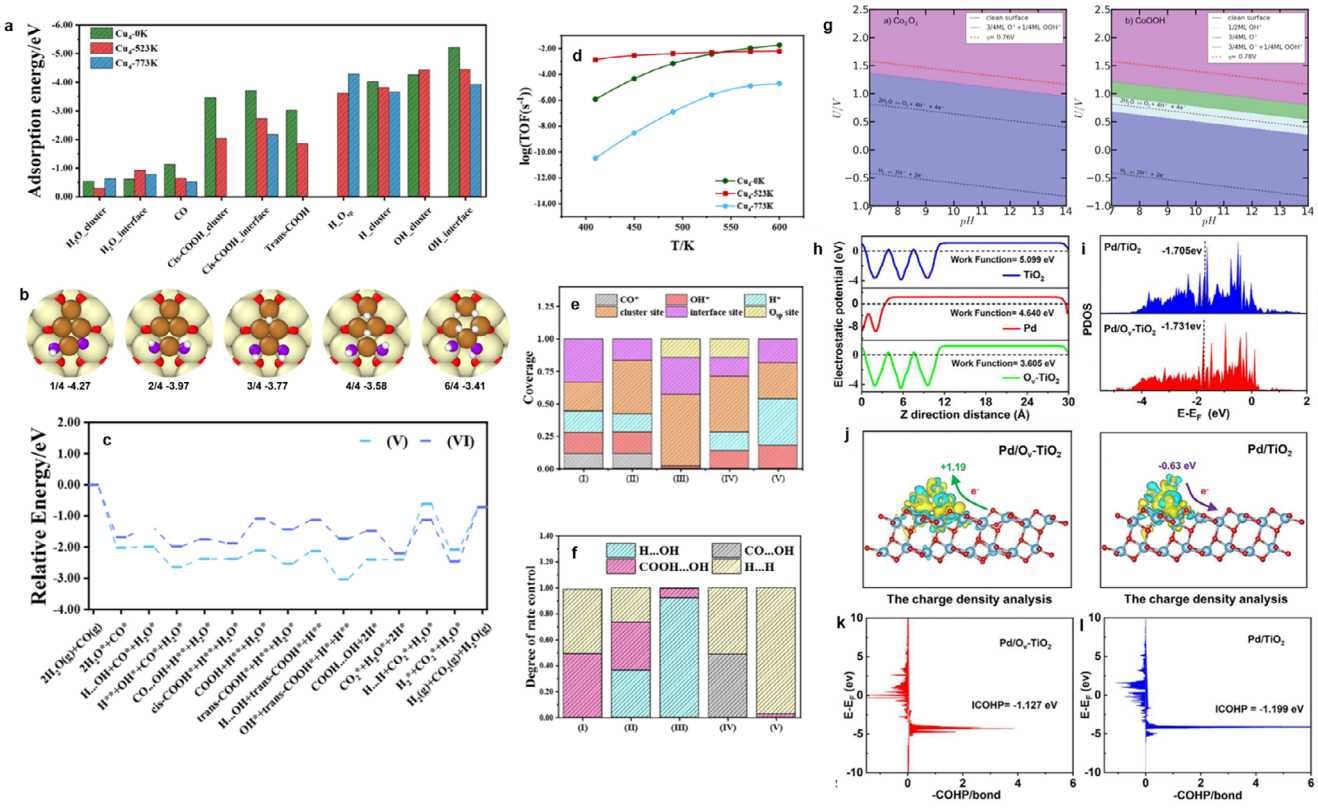

FIGURE 17 | (A) Plot of the adsorption energy of key species in the WGSR. (b) The coverage of hydrogen atoms and average adsorption energy in eV. (c) Difference in the relative energy diagram among WGSRs. (d) TOF plot. (e, f) Coverage chart and DRC plot of Cu/CeO_2 system [181]. Copyright 2025, American Chemical Society. (g) Surface Pourbaix diagram obtained from DFT+U calculations. (a) Co_3O_4 and (b) CoOOH [183] Copyright 2012, American Chemical Society. h) Work function estimated for TiO_2 (blue), Pd (red), and O_V-TiO_2 (green). (i) PDOS plots for Pd/O_V-TiO_2 and Pd/TiO_2. (j) Difference charge density analyses of Pd/O_V-TiO_2 and Pd/TiO_2. k) pCOHP of Pd/O_V-TiO_2 and Pd/TiO_2 [184] Copyright 2023, American Chemical Society.

different catalyst isomers to reactions, providing a more accurate reflection of catalyst dynamics under realistic conditions. AIMD's ability to incorporate quantum mechanical effects makes it an indispensable tool for understanding reaction mechanisms, especially for systems involving complex electronic interactions, charge transfer, or dynamic structural changes. By bridging the gap between electronic structure and macroscopic behavior, AIMD significantly enhances our capability to model and predict catalytic phenomena.

For example, Li et al. employed AIMD to investigate CO oxidation on ceria-supported gold clusters of varying sizes [193]. Their study revealed that single atoms dynamically form upon exposure to CO molecules and reintegrate into the cluster after the reaction is complete. This dynamic structural evolution provided critical insights into experimental results and the understanding of reaction mechanisms, as shown in Figure 18a,b. At the same time, the radial distribution functions and bond length distribution diagrams in Figure 18c,d also further demonstrate the impact of SMSI-driven dynamic evolution on the geometry of Au clusters. Speybroeck et al. used AIMD simulations to explore the dynamic evolution caused by SMSI within complex pore structures. They found that metal atoms in zeolite-based catalysts can be activated through interactions with adsorbates to form dynamic active sites. These findings emphasize the importance of catalyst structure design and highlight the role of dynamic processes in enhancing catalytic activity and selectivity [194, 195]. Liu et al. developed a QM/MM approach to simulate heterogeneous reactions under realistic conditions, incorporating factors such as temperature, pressure, and chemical environment [196]. They discovered that nanocatalysts are highly flexible under working conditions, with the dynamic evolution of their structures significantly influencing the free energy landscape of reactions, as shown in Figure 18e–g. Although AIMD has been successfully applied to investigate catalyst dynamics under reaction conditions, its high computational cost limits its applicability to relatively small catalytic systems, typically containing hundreds of atoms, and to time scales of only tens of picoseconds [197–199]. Consequently, AIMD is currently inefficient for studying the dynamic processes of realistic and complex heterogeneous catalysts.

Machine learning (ML) has recently emerged as a powerful alternative to traditional computational methods in materials science. While conventional approaches have provided fundamental insights into electronic structures and thermodynamics, they are often limited by high computational costs and long simulation times, particularly for large or complex systems. ML offers a data-driven framework that overcomes these limitations and accelerates the pace of materials discovery. The first advantage of ML is efficiency. Once trained on datasets generated from experiments or first-principles calculations, ML models can predict material properties several orders of magnitude faster

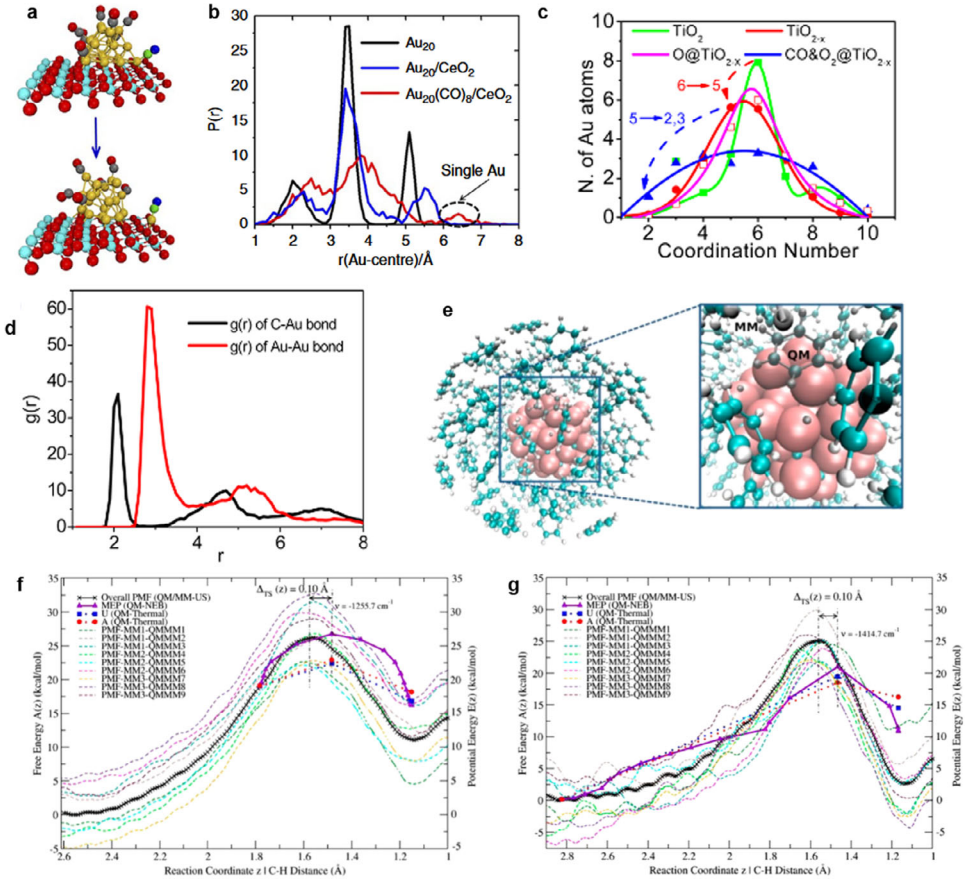

FIGURE 18 | (a) Initial and final configuration of the AIMD simulation for a $CeO_2(111)$ supported Au_{20} cluster with eight CO adsorption. (b) The probability distribution functions P(r) of the Au atoms relative to the centre-of-mass of the Au_{20} based on ~20 ps MD simulations at 700 K [10]. Copyright 2015, Springer Nature. (c) the statistical distribution curve of low coordinated Au atoms for Au_{20}/TiO_2, Au_{20}/TiO_{2-x}, and CO-Au_{20}/TiO_{2-x}. (d) The radio bond distributions for Au—C and Au—Au bonds. [200] Copyright 2013, American Chemical Society. (e) Schematic diagram of QM/MM model. (f,g) Calculation of free energy curves at different stages of hydrogenation reaction using QM/MM method [196]. Copyright 2015, American Chemical Society.

than traditional methods. This makes it possible to perform high-throughput screening across vast chemical spaces, enabling the rapid identification of promising candidates for catalysis, energy storage, and other electronic applications. ML-based interatomic potentials are especially valuable, as they achieve near DFT accuracy with the speed of classical force fields. Another advantage lies in adaptability. Unlike traditional methods constrained by approximations, ML can capture highly nonlinear and complex relationships between structure and properties without predefined functional forms. This flexibility enables the discovery of hidden correlations and allows the integration of diverse datasets, ranging from spectroscopy and microscopy experiments to computational databases. Moreover, ML extends predictive capability beyond conventional techniques. It can forecast long-term stability, defect dynamics, and catalytic performance under varying conditions-phenomena that are difficult to model with short timescale simulations. Active learning strategies further enhance efficiency by selectively adding the most informative data to refine models, reducing the need for exhaustive datasets.

Recently, machine learning methods, particularly machine learning potentials (MLPs), have emerged as promising tools for molecular modeling of catalyst dynamics [201–203]. Modern MLPs allow transferring the accuracy of first-principles electronic structure methods to large systems by constructing high-dimensional potential energy surfaces based on reference electronic structure calculations for representative atomic configurations using machine learning techniques, as shown in Figure 19a [204–206]. The algorithms underlying MLPs are still being actively optimized, with current efforts primarily focusing on improving computational efficiency, generalizability across diverse chemical environments, and the interpretability of the learned potential energy surfaces. For example, Yu et al. proposed a new MLP construction framework-MB-PIPNet, which successfully achieved a potential function model that can match the accuracy of the first principles while being highly integrated with the computational efficiency of the traditional molecular force field method. This study does not uses the traditional atomic energy expansion scheme; instead, chooses a new path to decompose the total potential energy of the complex system into the sum of the effective monomeric energy. This scheme enables the MB-PIPNet algorithm to have significant computational advantages while ensuring the model accuracy: the computational cost is proportional to the number of molecular monomers, and there is no need to introduce complex high-order descriptors, as shown in Figure 19b [207]. MLP-assisted MD simulations have now been successfully applied in the field of dynamic catalysis, enabling the exploration of catalyst structural evolution over longer time

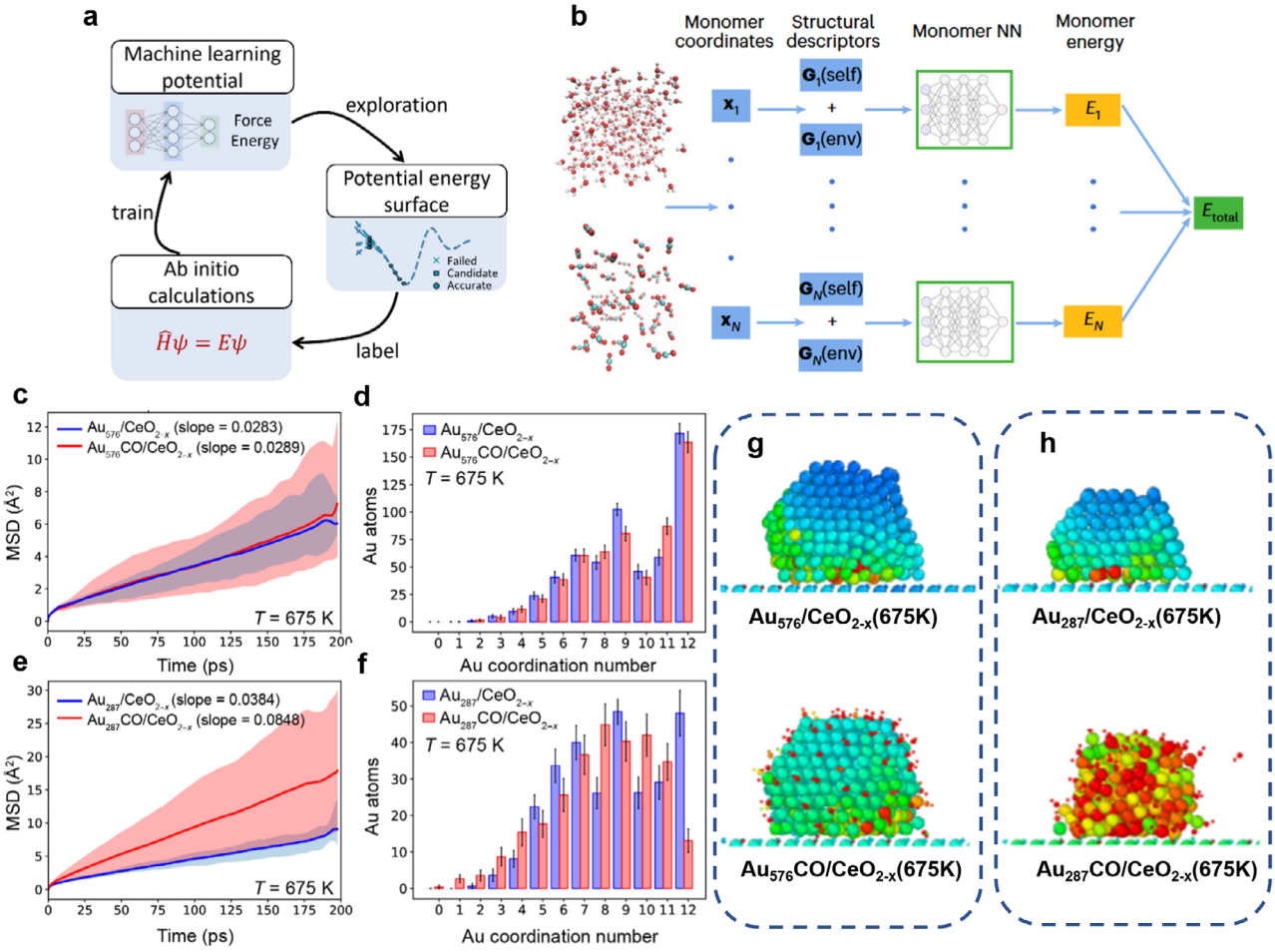

FIGURE 19 | (a) A machine learning workflow, which is composed of training of machine learning potential, exploration of configuration spaces, and data labeling by AIMD [169]. Copyright 2024, American Chemical Society. (b) Schematic of the MB-PIPNet architecture [207]. Copyright 2025, Springer Nature. (c–h) DPMD simulations of supported Au_{287} and Au_{576} NPs on defected CeO_2(111). (c,e) Corresponding MSDs averaged over five DPMD simulation trajectories. (d,f) Coordination number distribution of Au atoms without and with CO adsorption. (g,h) Colored local Lindemann index snapshots at 200 ps. (blue balls:FCC structure; red balls: disordered) [212]. Copyright 2024, The American Association for the Advancement of Science.

scales under reaction conditions [208]. Elias et al.'s study of ZnO-supported copper clusters and their extension to the ternary Cu/ZnO system using the HDNNPs method revealed a variety of structural patterns. Studies on copper-cerium (CuO/CeO_2) catalysts for low-temperature CO oxidation reactions have shown that surface-substituted $Cu_yCe_{1-y}O_{2-x}$ has higher catalytic activity than bulk CuO [209, 210]. In contrast to conventional AIMD simulations, Gong et al. demonstrated that machine learning-accelerated molecular dynamics maintains ab initio-level accuracy while enabling enhanced statistical sampling of reaction free energies on nanocatalysts. This approach substantially reduced computational costs, achieving accessible timescales extended to at least 20 ns, a two orders of magnitude advancement compared to the picosecond regime typical of traditional AIMD methods [211]. Liu et al. employed Deep Potential Molecular Dynamics (DeePMD) simulations to investigate the dynamic structural evolution of supported Au NPs with varying sizes under CO oxidation conditions. Their study revealed that in CO-rich environments, ultrasmall Au NPs exhibit a highly disordered atomic arrangement and undergo phase transformation, as shown in Figure 19c–h. Notably, this liquid-like configuration generates abundant reactive sites, enabling CO oxidation to proceed not only at the Au/CeO_2 interface but also directly on the solid-state Au NP surfaces. These findings have elucidated the pivotal role of size effects in governing the activity of noble metal catalysts and have provided critical insights for designing more efficient, atomically tailored nanocatalysts [212].

More broadly, the field is moving toward interpretable ML frameworks that bridge data-driven predictions with physical understanding. Interpretable models, such as those developed through symbolic regression or physically constrained neural networks, provide transparent mathematical relationships between fundamental parameters (such as adsorption energy, coordination number, and metal-support interaction strength) and catalytic activity. This shift from black-box learning to physics-aware modeling enables the establishment of universal design principles that link catalyst composition, surface structure, and reaction performance [213–215]. In the study by Li [5], although the core framework was established through kinetic simulations and scaling relations, the integration of first-principles neural network molecular dynamics demonstrated how machine

learning techniques could capture complex atomic processes at realistic time and length scales. This enabled the validation of the Sabatier principle of MSI, which states that an optimal MSI should be neither too strong nor too weak, thereby avoiding the competing destabilization pathways of Ostwald ripening and particle migration. High-throughput screening, empowered by these computational tools, revealed that heteroenergetic supports can substantially surpass the conventional stability limits, providing a universal guideline for designing catalysts with extended lifetimes. Building upon this foundation, Wang et al. [13] explicitly leveraged interpretable machine learning to construct a general MSI theory. By applying advanced symbolic regression to 178 experimentally measured adhesion energies, they discovered a predictive formula that connects MSI strength to fundamental physical descriptors, such as metal-oxygen and metal-metal interactions. Unlike black-box models, this interpretable approach ensured both accuracy and generalizability, while retaining a transparent physical meaning. Moreover, molecular dynamics simulations with global neural network potentials revealed that strong metal-metal interactions, rather than oxophilicity alone, govern the encapsulation processes of supported catalysts. The derived principle was confirmed across 10 late transition metals and 16 oxides, offering a comprehensive framework for understanding strong MSIs and their impact on catalyst stability and performance.

It is important to note that machine learning cannot yet operate independently from DFT calculations, as it still lacks the quantum-mechanical foundation and generalizability that underpin first-principles methods. The true strength of machine learning lies in its integration with traditional computational approaches, enabling greater efficiency and intelligence in materials research. In the field of catalysis, this synergy between accuracy and computational speed allows machine learning to play a transformative role-accelerating the discovery and validation of fundamental phenomena, facilitating predictive catalyst design, and reducing reliance on conventional trial-and-error strategies. Future theoretical efforts will focus on developing more accurate and transferable potential energy functions to describe complex catalytic environments. In addition, the development of multiscale simulation frameworks that bridge electronic, atomic, and reactor-level processes c emerging quantum computing techniques will further improve both the accuracy and efficiency of theoretical simulations.

The advent of data-driven modeling and advanced experimental characterization techniques has profoundly transformed the understanding of SMSI. Traditionally, SMSI was interpreted primarily through static surface models derived from ex situ microscopy or spectroscopy, limiting insights into its dynamic and reversible nature under reaction conditions. With the development of machine learning assisted data analytics and in situ/operando characterization tools, such as transmission electron microscopy (TEM), X-ray absorption spectroscopy (XANES/EXAFS), and X-ray photoelectron spectroscopy, researchers can now directly observe atomic scale structural and electronic evolutions of catalysts during operation. ML algorithms are capable of extracting latent correlations between structural descriptors and catalytic behavior from high-dimensional datasets, thereby overcoming the limitations of manual interpretation. For instance, deep-learning frameworks have automated TEM image analysis to trace atomic migration and encapsulation processes characteristic of SMSI, while neural network and regression models applied to time-resolved XANES have revealed charge redistribution and oxidation state dynamics at the metal-support interface. These combined approaches provide a quantitative, dynamic picture of SMSI, linking transient interfacial electronic reconstruction to catalytic performance. Consequently, data-driven modeling integrated with advanced characterization has shifted the paradigm from static qualitative descriptions to real-time, quantitative, and interpretable mechanistic understanding, revealing that SMSI is not a fixed structural phenomenon but a dynamic and tunable interfacial process governed by electronic and thermodynamic feedback during catalysis.

In recent years, artificial intelligence technology has developed rapidly. In addition to the development of new paradigms for theoretical computation accelerated by machine learning, automated laboratory workflows integrated with large language models (AI chemists) are another promising research prospect. For example, Jiang et al. recently developed a robotic AI chemist powered by a hierarchical multi-agent system, ChemAgents, based on an onboard Llama-3.1–70B LLM, which can perform complex multi-step experiments with minimal human intervention, fully integrating literature review, experimental design, computational execution, and experimental operation [216]. Unlike the machine learning research by Li et al. mentioned above, AI chemists can not only achieve high-throughput screening of novel SMSI systems, but also automatically control and test experimental parameters, potentially becoming the next-generation research paradigm. In other words, heterogeneous SMSI catalysts have complex structures and diverse construction strategies, and research on them has primarily relied on traditional trial-and-error methods. The emergence of machine learning theory has, on the one hand, broken through the computational limitations of traditional DFT methods, and on the other hand, predicted and screened potential adaptable SMSI structures. AI-driven automated experimental workflows have further improved research methods from theoretical prediction to experimental verification, enabling high-throughput experimental construction and SMSI testing based on effective theoretical predictions. This has accelerated the research process of novel catalysts and promoted the development of closed-loop catalyst design systems that can independently propose, synthesize, and evaluate materials [217, 218].

5 | Conclusion and Perspective

The phenomenon of strong metal-support interactions (SMSI) has garnered significant attention over the past decade, with emerging discoveries providing novel principles for regulating the selectivity, activity, and stability of heterogeneous catalysts. In addition to robust interfacial electron transfer, the formation and redispersion of encapsulated structures have become widely accepted features of SMSI. The feature of SMSI is defined as the formation of robust interfacial metal–metal bonds with shorter bond lengths than those observed in intermetallic compounds. While the formation mechanism remains incompletely understood, the surface energy minimization hypothesis offers the most plausible explanation. At elevated temperatures, active metals

typically exhibit higher surface energy than the support, allowing the activated support to gradually migrate and cover the surface of the active metal, minimizing the surface energy.

The SMSI mechanism induces atomic rearrangements and charge redistribution, providing multiple avenues for modifying the unique surface structure of heterogeneous catalysts and improving catalytic performance. Through the SMSI effect, researchers can independently manipulate the composition and structure of the active metal phase and support phase, or control reaction conditions, thereby exploiting the SMSI structure to rationally design catalysts for specific reactions.

Recent advances in in situ and operando characterization techniques, combined with progress in theoretical simulations, have greatly deepened our understanding of SMSI. The development of environmental transmission electron microscopy (ETEM), near-ambient pressure X-ray photoelectron spectroscopy (NAP-XPS), and synchrotron-based X-ray absorption spectroscopy (XAS) has enabled real-time monitoring of metal-support interfacial evolution under realistic conditions, revealing dynamic processes such as reversible encapsulation, metal migration, and oxidation-state transitions. Meanwhile, advances in density functional theory (DFT), ab initio molecular dynamics (AIMD), and machine-learning-accelerated simulations have provided atomic-level insights into charge redistribution, adsorption energetics, and interfacial reconstruction, offering a theoretical foundation for the interpretation of experimental observations.

Despite these advances, major challenges remain. It is still difficult to capture transient atomic processes under realistic high-temperature and high-pressure environments, as the spatial and temporal resolution of current techniques remain limited. The high precision requirements and cost of instrumentation restrict broader application, while the coupling of geometric, electronic, and interfacial migration effects complicate data interpretation. On the theoretical side, achieving a balance between accuracy and computational cost remains a major bottleneck, as obtaining reliable electronic structures and reaction pathways continues to require substantial computational resources.

Future progress in SMSI research will rely on developing operando-compatible systems with higher spatial and temporal resolution, enabling atomic-level visualization of interfacial dynamics under realistic catalytic conditions. Future theoretical efforts will focus on developing more accurate and transferable potential energy functions to describe complex catalytic environments. In addition, the integration of multiscale modeling and emerging quantum computing techniques will further improve both the accuracy and efficiency of theoretical simulations. At the same time, the interdisciplinary integration of advanced characterization and theoretical modeling is essential. Combining AIMD with in situ environmental TEM or coupling in situ spectroscopy with DFT can provide complementary insights into charge transfer, atomic diffusion, and interfacial reconstruction. Beyond this, the rise of AI chemists marks a transformative step for catalyst research. Artificial intelligence-driven automated experimental platforms can autonomously design, synthesize, and evaluate novel SMSI catalysts, effectively establishing a closed-loop research framework that links theoretical prediction, high-throughput synthesis, and experimental validation. This paradigm shift will not only accelerate the discovery of adaptive SMSI structures but also advance the intelligent evolution of catalyst design.

In conclusion, SMSI represents a powerful paradigm for tailoring heterogeneous catalysts at atomic scales. By bridging fundamental understanding with synthetic innovation, SMSI-driven strategies hold transformative potential for next-generation catalyst design, particularly in achieving high-density active site configurations and precise electronic state control. Future research should prioritize establishing universal SMSI design principles while expanding its applicability to emerging energy conversion systems.

Acknowledgements

C.L. greatly appreciates the financial provided by the National Natural Science Foundation of China (Grant Number. 22473108), the foundation of China's National Key R&D Programme (Grant Number. 2023YFB3810601), and the Hundred Talents Program of CAS. Y.W. Thanks the Team Construction Project of Liaoning Province Education Department (Grant Number. LJ222410164013), and Liaoning Provincial Natural Science Foundation (Grant Number. 2024-MS-224).

Conflicts of Interest

The authors declare no conflict of interest.

Data Availability Statement

The authors have nothing to report.

References

1. A. H. Motagamwala, R. Almallahi, J. Wortman, V. O. Igenegbai, and S. Linic, "Stable and Selective Catalysts for Propane Dehydrogenation Operating at Thermodynamic Limit," *Science* 373 (2021): 217–222.

2. C. A. Salazar, K. N. Flesch, B. E. Haines, P. S. Zhou, D. G. Musaev, and S. S. Stahl, "Tailored Quinones Support High-turnover Pd Catalysts for Oxidative C–H Arylation with O 2," *Science* 370 (2020): 1454–1460.

3. X.-Y. He, Y.-Z. Liu, J.-J. Chen, X. Lan, X.-N. Li, and S.-G. He, "Size-Dependent Reactivity of Co n– (n = 5–25) Cluster Anions toward Carbon Dioxide," *The Journal of Physical Chemistry Letters* 14 (2023): 6948–6955.

4. X. Li, S. Mitchell, Y. Fang, J. Li, J. Perez-Ramirez, and J. Lu, "Advances in Heterogeneous Single-cluster Catalysis," *Nature Reviews Chemistry* 7 (2023): 754–767.

5. S. Hu and W.-X. Li, "Sabatier Principle of Metal-support Interaction for Design of Ultrastable Metal Nanocatalysts," *Science* 374 (2021): 1360–1365.

6. G. Zhao, P. Li, N. Cheng, S. X. Dou, and W. Sun, "An Ir/Ni(OH) 2 Heterostructured Electrocatalyst for the Oxygen Evolution Reaction: Breaking the Scaling Relation, Stabilizing Iridium(V), and Beyond," *Advanced Materials* 32 (2020): 2000872.

7. R. Lang, X. Du, Y. Huang, et al., "Single-Atom Catalysts Based on the Metal–Oxide Interaction," *Chemical Reviews* 120 (2020): 11986–12043.

8. S. Praserthdam, S. Somdee, M. Rittiruam, and P. B. Balbuena, "Computational Study of the Evolution of Ni-Based Catalysts during the Dry Reforming of Methane," *Energy & Fuels* 34 (2020): 4855–4864.

9. H.-M. Yan, G. Wang, X.-M. Lv, H. Cao, G.-Q. Qin, and Y.-G. Wang, *Journal of the American Chemical Society* 147 (2025): 3274.

10. Y.-G. Wang, D. Mei, V.-A. Glezakou, J. Li, and R. Rousseau, "Dynamic Formation of Single-atom Catalytic Active Sites on Ceria-supported Gold Nanoparticles," *Nature Communications* 6 (2015): 6511.

11. K. Murata, A. Oda, A. Satsuma, and K. Sawabe, "Unveiling Static and Dynamic Structures of Pd Clusters Influenced by Al 2 O 3 Surfaces: DFT and AIMD Studies," *The Journal of Physical Chemistry C* 127 (2023): 20267–20275.

12. X. Wu, X. Fan, S. Xie, et al., "Zinc-indium-sulfide Favors Efficient C – H Bond Activation by Concerted Proton-coupled Electron Transfer," *Nature Communications* 15 (2024): 4967.

13. T. Wang, J. Hu, R. Ouyang, et al., "Nature of Metal-support Interaction for Metal Catalysts on Oxide Supports," *Science* 386 (2024): 915–920.

14. S. J. Tauster, S. C. Fung, and R. L. Garten, "Strong Metal-support Interactions. Group 8 Noble Metals Supported on Titanium Dioxide," *Journal of the American Chemical Society* 100 (1978): 170–175.

15. S. C. Fung, "XPS Studies of Strong Metal-support Interactions (SMSI)?Pt/TiO2," *Journal of Catalysis* 76 (1982): 225–230.

16. M. K. Bahl, S. C. Tsai, and Y. W. Chung, "Auger and Photoemission Investigations of the Platinum-SrTi O3 (100) Interface: Relaxation and Chemical-shift Effects," *Physical Review B* 21 (1980): 1344–1348.

17. R. A. Demmin, C. S. Ko, and R. J. Gorte, "Effect of Titania on the Chemisorption and Reaction Properties of Platinum," *The Journal of Physical Chemistry* 89 (1985): 1151–1154.

18. D. N. Belton, Y. M. Sun, and J. M. White, "Thin-film Models of Strong Metal-support Interaction Catalysts. Platinum on Oxidized Titanium," *The Journal of Physical Chemistry* 88 (1984): 1690–1695.

19. S. Sakellson, M. McMillan, and G. L. Haller, "EXAFS Evidence for Direct Metal-metal Bonding in Reduced Rhodium/Titania Catalysts," *The Journal of Physical Chemistry* 90 (1986): 1733–1736.

20. S. J. Tauster, "Strong Metal-support Interactions," *Accounts of Chemical Research* 20 (1987): 389–394.

21. A. Bruix, J. A. Rodriguez, P. J. Ramírez, et al., "A New Type of Strong Metal–Support Interaction and the Production of H 2 through the Transformation of Water on Pt/CeO 2 (111) and Pt/CeO X/TiO 2 (110) Catalysts," *Journal of the American Chemical Society* 134 (2012): 8968–8974.

22. Y. Guo, S. Mei, K. Yuan, et al., "Low-Temperature CO 2 Methanation over CeO 2 -Supported Ru Single Atoms, Nanoclusters, and Nanoparticles Competitively Tuned by Strong Metal–Support Interactions and H-Spillover Effect," *ACS Catalysis* 8 (2018): 6203–6215.

23. K. Kunimori, K. Ito, K. Iwai, and T. Uchijima, "Strong Metal-Support Interaction (SMSI) BEHAVIOR of Rh/Nb2O5 Catalyst Studied By Ethane Hydrogenolysis And Hydrogen Chemisorption," *Chemistry Letters* 15 (1986): 573–576.

24. J. Dong, Q. Fu, H. Li, et al., "Reaction-Induced Strong Metal–Support Interactions between Metals and Inert Boron Nitride Nanosheets," *Journal of the American Chemical Society* 142 (2020): 17167–17174.

25. S. Wang, M. Fan, H. Pan, et al., "Achieving Asymmetric Redox Chemistry for Oxygen Evolution Reaction through Strong Metal-support Interactions," *Journal of Energy Chemistry* 96 (2024): 526–535.

26. S. Zhang, P. N. Plessow, J. J. Willis, et al., "Dynamical Observation and Detailed Description of Catalysts under Strong Metal–Support Interaction," *Nano Letters* 16 (2016): 4528–4534.

27. Y. Lou, J. Xu, Y. Zhang, C. Pan, Y. Dong, and Y. Zhu, "Metal-support Interaction for Heterogeneous Catalysis: from Nanoparticles to Single Atoms," *Materials Today Nano* 12 (2020): 100093.

28. Z. Luo, G. Zhao, H. Pan, and W. Sun, "Strong Metal–Support Interaction in Heterogeneous Catalysts," *Advanced Energy Materials* 12 (2022): 2201395.

29. W. Guo, H. Su, G. Zhao, H. Pan, and W. Sun, "The Principles behind Different Forms of Strong Metal-Support Interaction in Heterogeneous Catalysts," *Advanced Functional Materials* (2025): 12002.

30. H. Wang, Z. Gao, B. Sun, et al., *Chem Catal* 3 (2023): 100768.

31. R. Burch and A. R. Flambard, "Strong Metal-support Interactions in Nickel/Titania Catalysts: the Importance of Interfacial Phenomena," *Journal of Catalysis* 78 (1982): 389–405.

32. S. E. Golunski, H. A. Hatcher, R. R. Rajaram, and T. J. Truex, "Origins of Low-temperature Three-way Activity in Pt/CeO2," *Applied Catalysis B: Environmental* 5 (1995): 367–376.

33. Y. He, J. Zhang, F. Polo-Garzon, and Z. Wu, "Adsorbate-Induced Strong Metal–Support Interactions: Implications for Catalyst Design," *The Journal of Physical Chemistry Letters* 14 (2023): 524–534.

34. F. Qi, J. Peng, Z. Liang, et al., *Environ Sci Ecotech* 22 (2024): 100443.

35. A. Corma, P. Serna, P. Concepción, and J. J. Calvino, "Transforming Nonselective into Chemoselective Metal Catalysts for the Hydrogenation of Substituted Nitroaromatics," *Journal of the American Chemical Society* 130 (2008): 8748–8753.

36. M. C. J. Bradford and M. A. Vannice, "Catalytic Reforming of Methane with Carbon Dioxide over Nickel Catalysts I. Catalyst Characterization and Activity," *Applied Catalysis A: General* 142 (1996): 73–96.

37. C. M. Y. Yeung, K. M. K. Yu, Q. J. Fu, D. Thompsett, M. I. Petch, and S. C. Tsang, "Engineering Pt in Ceria for a Maximum Metal−Support Interaction in Catalysis," *Journal of the American Chemical Society* 127 (2005): 18010–18011.

38. Q. Fu and T. Wagner, "Interaction of Nanostructured Metal Overlayers with Oxide Surfaces," *Surface Science Reports* 62 (2007): 431–498.

39. S. J. Tauster, S. C. Fung, R. T. K. Baker, and J. A. Horsley, "Strong Interactions in Supported-Metal Catalysts," *Science* 211 (1981): 1121–1125.

40. Z. Hou, C. Cui, Y. Yang, et al., "Strong Metal-Support Interactions in Heterogeneous Oxygen Electrocatalysis," *Small* 20 (2024): 2407167.

41. H. Xu, J. Z. Zhu, C. Zou, et al., *Energy&Fuels* 37 (2023): 16781–16789.

42. H. Tang, Y. Su, B. Zhang, et al., "Classical Strong Metal–support Interactions between Gold Nanoparticles and Titanium Dioxide," *Science Advances* 3 (2017): 1700231.

43. S. Zhang, P. N. Plessow, J. J. Willis, et al., "Dynamical Observation and Detailed Description of Catalysts under Strong Metal–Support Interaction," *Nano Letters* 16 (2016): 4528–4534.

44. L. Wang, J. Zhang, Y. Zhu, et al., "Strong Metal–Support Interactions Achieved by Hydroxide-to-Oxide Support Transformation for Preparation of Sinter-Resistant Gold Nanoparticle Catalysts," *ACS Catalysis* 7 (2017): 7461–7465.

45. H. Tang, J. Wei, F. Liu, et al., "Strong Metal–Support Interactions between Gold Nanoparticles and Nonoxides," *Journal of the American Chemical Society* 138 (2016): 56–59.

46. J. C. Matsubu, S. Zhang, L. DeRita, et al., "Adsorbate-mediated Strong Metal–support Interactions in Oxide-supported Rh Catalysts," *Nature Chemistry* 9 (2017): 120–127.

47. S. Liu, W. Xu, Y. Niu, et al., "Ultrastable Au Nanoparticles on Titania through an Encapsulation Strategy under Oxidative Atmosphere," *Nature Communications* 10 (2019): 5790.

48. X. Teng, D. Si, L. Chen, and J. Shi, "Synergetic Catalytic Effects by Strong Metal–support Interaction for Efficient Electrocatalysis," *Escience* 4 (2024): 100272.

49. F. Qi, J. Peng, Z. Liang, et al., "Strong Metal-support Interaction (SMSI) in Environmental Catalysis: Mechanisms, Application, Regulation Strategies, and Breakthroughs," *Environmental Science and Ecotechnology* 22 (2024): 100443.

50. A. S. Ivanova, E. M. Slavinskaya, R. V. Gulyaev, et al., *Applied Catalysis B: Environment and Energy* 97 (2010): 57–71.

51. S. Khatiri Nejad Fard and A. Besharati-Seidani, "Optimization of Pd/Al2O3 Catalysts Preparation and Process Conditions Catalysts for the Removal of Hydrogen from Air," *Fuel* 396 (2025): 135252.

52. N. Daelman, M. Capdevila-Cortada, and N. López, "Dynamic Charge and Oxidation state of Pt/CeO2 Single-atom Catalysts," *Nature Materials* 18 (2019): 1215–1221.

53. M. Xue, B. Wang, M. Fan, L. Ling, and R. Zhang, "Ethane Oxidative Dehydrogenation over TiO 2 and M/TiO 2 Catalysts: Unraveling the Sur-

face Structure Evolution, Oxygen Species Type, and Role of Doped Metal in Tuning Catalytic Performance," *ACS Catalysis* 15 (2025): 2095–2109.

54. V. Bernales, D. Yang, J. Yu, et al., "Molecular Rhodium Complexes Supported on the Metal-Oxide-Like Nodes of Metal Organic Frameworks and on Zeolite HY: Catalysts for Ethylene Hydrogenation and Dimerization," *ACS Applied Materials & Interfaces* 9 (2017): 33511–33520.

55. T. He, S. Chen, B. Ni, et al., "Zirconium–Porphyrin-Based Metal–Organic Framework Hollow Nanotubes for Immobilization of Noble-Metal Single Atoms," *Angewandte Chemie International Edition* 57 (2018): 3493–3498.

56. T. Sun, L. Xu, D. Wang, and Y. Li, "Metal Organic Frameworks Derived Single Atom Catalysts for Electrocatalytic Energy Conversion," *Nano Research* 12 (2019): 2067–2080.

57. Y. Yu, X. Cui, Y. Hong, G. Qin, and S. Li, "Efficient Electrosynthesis of CO-rich Syngas over CeO2-armored Ag Nanowires toward Sustainable Steelmaking," *Applied Catalysis B: Environment and Energy* 373 (2025): 125352.

58. H. O. Otor, J. B. Steiner, C. García-Sancho, and A. C. Alba-Rubio, "Encapsulation Methods for Control of Catalyst Deactivation: a Review," *ACS Catalysis* 10 (2020): 7630–7656.

59. Q. Fu, T. Wagner, S. Olliges, and H.-D. Carstanjen, "Metal−Oxide Interfacial Reactions: Encapsulation of Pd on TiO 2 (110)," *The Journal of Physical Chemistry B* 109 (2005): 944–951.

60. A. Beck, X. Huang, L. Artiglia, et al., "The Dynamics of Overlayer Formation on Catalyst Nanoparticles and Strong Metal-support Interaction," *Nature Communications* 11 (2020): 3220.

61. J. A. Horsley, "A Molecular Orbital Study of Strong Metal-support Interaction between Platinum and Titanium Dioxide," *Journal of the American Chemical Society* 101 (1979): 2870–2874.

62. J. W. M. Crawley, I. E. Gow, N. Lawes, et al., "Heterogeneous Trimetallic Nanoparticles as Catalysts," *Chemical Reviews* 122 (2022): 6795–6849.

63. C. Gao, F. Lyu, and Y. Yin, "Encapsulated Metal Nanoparticles for Catalysis," *Chemical Reviews* 121 (2021): 834–881.

64. H. Wang, L. Wang, D. Lin, et al., "Strong Metal–support Interactions on Gold Nanoparticle Catalysts Achieved through Le Chatelier's Principle," *Nature Catalysis* 4 (2021): 418–424.

65. X. Liu, M.-H. Liu, Y.-C. Luo, et al., "Strong Metal–Support Interactions between Gold Nanoparticles and ZnO Nanorods in CO Oxidation," *Journal of the American Chemical Society* 134 (2012): 10251–10258.

66. C. Dong, Z. Gao, Y. Li, et al., "Fully Exposed Palladium Cluster Catalysts Enable Hydrogen Production from Nitrogen Heterocycles," *Nature Catalysis* 5 (2022): 485–493.

67. H. Xiong, S. Lin, J. Goetze, et al., "Thermally Stable and Regenerable Platinum–Tin Clusters for Propane Dehydrogenation Prepared by Atom Trapping on Ceria," *Angewandte Chemie* 129 (2017): 9114–9119.

68. A. Wang, J. Li, and T. Zhang, "Heterogeneous Single-atom Catalysis," *Nature Reviews Chemistry* 2 (2018): 65–81.

69. Z. Li, S. Ji, Y. Liu, et al., "Well-Defined Materials for Heterogeneous Catalysis: from Nanoparticles to Isolated Single-Atom Sites," *Chemical Reviews* 120 (2020): 623–682.

70. M. A. Newton, "Dynamic Adsorbate/Reaction Induced Structural Change of Supported Metal Nanoparticles: Heterogeneous Catalysis and beyond," *Chemical Society Reviews* 37 (2008): 2644.

71. H. Yang, P. Duan, Z. Zhuang, et al., "Understanding the Dynamic Evolution of Active Sites among Single Atoms, Clusters, and Nanoparticles," *Advanced Materials* 37 (2025): 2415265.

72. Y. Gao and B. Zhu, "Simulating Structural Dynamics of Metal Catalysts under Operative Conditions," *The Journal of Physical Chemistry Letters* 15 (2024): 8351–8359.

73. C. Dessal, T. Len, F. Morfin, et al., "Dynamics of Single Pt Atoms on Alumina during CO Oxidation Monitored by Operando X-ray and Infrared Spectroscopies," *ACS Catalysis* 9 (2019): 5752–5759.

74. S. Li, X. Luo, Y. Wang, et al., "Strong Oxide-Support Interaction Induced Thermal Stabilization of Pt Single Atoms for Durable Catalytic CO Oxidation," *Angewandte Chemie International Edition* 64 (2025): 202504551.

75. Y. Qin, W. Zhao, C. Xia, et al., "CO Intermediate-Assisted Dynamic Cu Sintering during Electrocatalytic CO 2 Reduction on Cu−N−C Catalysts," *Angewandte Chemie International Edition* 63 (2024): 202404763.

76. X. Bai, X. Zhao, Y. Zhang, et al., "Dynamic Stability of Copper Single-Atom Catalysts under Working Conditions," *Journal of the American Chemical Society* 144 (2022): 17140–17148.

77. S. Wei, A. Li, J.-C. Liu, et al., "Direct Observation of Noble Metal Nanoparticles Transforming to Thermally Stable Single Atoms," *Nature Nanotechnology* 13 (2018): 856–861.

78. A. J. Martín, S. Mitchell, C. Mondelli, S. Jaydev, and J. Pérez-Ramírez, *Nat Catal* 5 (2022): 854.

79. T. W. van Deelen, C. Hernández Mejía, and K. P. de Jong, "Control of Metal-support Interactions in Heterogeneous Catalysts to Enhance Activity and Selectivity," *Nature Catalysis* 2 (2019): 955–970.

80. J. Zhang, H. Wang, L. Wang, et al., "Wet-Chemistry Strong Metal–Support Interactions in Titania-Supported Au Catalysts," *Journal of the American Chemical Society* 141 (2019): 2975–2983.

81. A. Berkó, I. Ulrych, and K. C. Prince, *Journal of Physical Chemistry B* 102 (1998): 3379.

82. Y. Lei, F. Mehmood, S. Lee, et al., "Increased Silver Activity for Direct Propylene Epoxidation via Subnanometer Size Effects," *Science* 328 (2010): 224–228.

83. S. Vajda and M. G. White, "Catalysis Applications of Size-Selected Cluster Deposition," *ACS Catalysis* 5 (2015): 7152–7176.

84. H. Prats and M. Stamatakis, "Atomistic and Electronic Structure of Metal Clusters Supported on Transition Metal Carbides: Implications for Catalysis," *Journal of Materials Chemistry A* 10 (2022): 1522–1534.

85. E. Jimenez-Izal and A. N. Alexandrova, "Computational Design of Clusters for Catalysis," *Annual Review of Physical Chemistry* 69 (2018): 377–400.

86. Y. Zhang, J. Liu, K. Qian, et al., "Structure Sensitivity of Au-TiO 2 Strong Metal–Support Interactions," *Angewandte Chemie International Edition* 60 (2021): 12074–12081.

87. J. H. Kwak, L. Kovarik, and J. Szanyi, "CO 2 Reduction on Supported Ru/Al 2 O 3 Catalysts: Cluster Size Dependence of Product Selectivity," *ACS Catalysis* 3 (2013): 2449–2455.

88. J. H. Kwak, L. Kovarik, and J. Szanyi, "Heterogeneous Catalysis on Atomically Dispersed Supported Metals: CO 2 Reduction on Multifunctional Pd Catalysts," *ACS Catalysis* 3 (2013): 2094–2100.

89. J. C. Matsubu, V. N. Yang, and P. Christopher, "Isolated Metal Active Site Concentration and Stability Control Catalytic CO 2 Reduction Selectivity," *Journal of the American Chemical Society* 137 (2015): 3076–3084.

90. K. W. Ting, Z. Maeno, S. M. Siddiki, K. Shimizu, and T. Toyao, "Reverse Water-Gas Shift Reaction via Redox of Re Nanoclusters Supported on TiO2," *Chemistry Letters* 50 (2021): 158–161.

91. H. C. Wu, Y. C. Chang, J. H. Wu, J. H. Lin, I. K. Lin, and C. S. Chen, "Methanation of CO 2 and Reverse Water Gas Shift Reactions on Ni/SiO 2 Catalysts: the Influence of Particle Size on Selectivity and Reaction Pathway," *Catalysis Science & Technology* 5 (2015): 4154–4163.

92. X. Chen, X. Su, H. Duan, B. Liang, Y. Huang, and T. Zhang, "Catalytic Performance of the Pt/TiO2 Catalysts in Reverse Water Gas Shift Reaction: Controlled Product Selectivity and a Mechanism Study," *Catalysis Today* 281 (2017): 312–318.

93. H. Xin, L. Lin, R. Li, et al., "Overturning CO 2 Hydrogenation Selectivity with High Activity via Reaction-Induced Strong Metal–Support Interactions," *Journal of the American Chemical Society* 144 (2022): 4874–4882.

94. W. T. Figueiredo, G. B. Della Mea, M. Segala, et al., *American Chemical Society Applied Nano Materials* 2 (2019): 2559–2573.

95. L. Zhang, X. Liu, H. Wang, et al., "Size-dependent Strong Metal–support Interaction in Pd/ZnO Catalysts for Hydrogenation of CO 2 to Methanol," *Catalysis Science & Technology* 11 (2021): 4398–4405.

96. S. Kaiser, J. Plansky, M. Krinninger, et al., "Does Cluster Encapsulation Inhibit Sintering? Stabilization of Size-Selected Pt Clusters on Fe 3 O 4 (001) by SMSI," *ACS Catalysis* 13 (2023): 6203–6213.

97. P. Zhou, X. Hou, Y. Chao, et al., "Synergetic Interaction between Neighboring Platinum and Ruthenium Monomers Boosts CO Oxidation," *Chemical Science* 10 (2019): 5898–5905.

98. M. Liu, H. Chun, T.-C. Yang, et al., "Tuning the Site-to-Site Interaction in Ru–M (M = Co, Fe, Ni) Diatomic Electrocatalysts to Climb up the Volcano Plot of Oxygen Electroreduction," *ACS Nano* 16 (2022): 10657–10666.

99. H. Shi, H. Wang, Y. Zhou, et al., "Atomically Dispersed Indium-Copper Dual-Metal Active Sites Promoting C−C Coupling for CO 2 Photoreduction to Ethanol," *Angewandte Chemie International Edition* 61 (2022): 202208904.

100. K. Harrath, Z. Yao, Y.-F. Jiang, Y.-G. Wang, and J. Li, "Activity Origin of the Nickel Cluster on TiC Support for Nonoxidative Methane Conversion," *The Journal of Physical Chemistry Letters* 14 (2023): 4033–4041.

101. J. Yan, P. Zhang, D. Chen, et al., "First-principles Methods for Unraveling the Structure–catalytic Activity Relationship and Mechanism of δ-MnO 2 -supported Metal Cluster Catalysts in Ambient Temperature Benzene to CO 2 Degradation," *Nanoscale* 17 (2025): 9253–9261.

102. Z. Wu, Y. Li, and W. Huang, "Size-Dependent Pt-TiO 2 Strong Metal–Support Interaction," *The Journal of Physical Chemistry Letters* 11 (2020): 4603–4607.

103. C. Dong, Z. Gao, Y. Li, et al., "Fully Exposed Palladium Cluster Catalysts Enable Hydrogen Production from Nitrogen Heterocycles," *Nature Catalysis* 5 (2022): 485–493.

104. X. Zheng, Y. Liu, and Y. Yao, "Trimetallic Single-cluster Catalysts for Electrochemical Nitrogen Reduction Reaction: Activity Prediction, Mechanism, and Electronic Descriptor," *Chemical Engineering Journal* 426 (2021): 130745.

105. Y. Liu, J.-C. Liu, T.-H. Li, et al., "Unravelling the Enigma of Nonoxidative Conversion of Methane on Iron Single-Atom Catalysts," *Angewandte Chemie International Edition* 59 (2020): 18586–18590.

106. L. Song, X. Cao, and L. Li, "Engineering Stable Surface Oxygen Vacancies on ZrO 2 by Hydrogen-Etching Technology: an Efficient Support of Gold Catalysts for Water-Gas Shift Reaction," *ACS Applied Materials & Interfaces* 10 (2018): 31249–31259.

107. Y. Tang, Z. Liu, R. Ye, et al., "Selectively Located Pt Clusters on Au/CeO2 for Highly Robust Water-gas Shift Reaction via Atomic Layer Deposition," *Applied Catalysis B: Environment and Energy* 356 (2024): 124218.

108. X. Cai, X. Liu, X. Wei, and R. Lin, "Effect of Nitrogen-Doped Carbon Support on the Performance of Catalysts for the Oxygen Reduction Reaction," *ACS Applied Energy Materials* 7 (2024): 8705–8714.

109. K. Murata, A. Oda, A. Satsuma, and K. Sawabe, "Unveiling Static and Dynamic Structures of Pd Clusters Influenced by Al 2 O 3 Surfaces: DFT and AIMD Studies," *The Journal of Physical Chemistry C* 127 (2023): 20267–20275.

110. E. M. Slavinskaya, O. A. Stonkus, R. V. Gulyaev, et al., *Applied Catalysis A: General* 401 (2011): 83–97.

111. Y. Gao, W. Sun, W. Yang, and Q. Li, "Creation of Pd/Al2O3 Catalyst by a Spray Process for Fixed Bed Reactors and Its Effective Removal of Aqueous Bromate," *Scientific Reports* 7 (2017): 41797.

112. A. S. Ivanova, E. M. Slavinskaya, R. V. Gulyaev, et al., *Applied Catalysis B: Environmental* 97 (2010): 57–71.

113. Y. Pu, Y. Niu, Y. Wang, Q. Liang, L. Zhang, and B. Zhang, "Sinter Resistance and Activity Enhancement via a Facet-Dependent Metal–Support Interaction of Pd/ZnO Catalysts in CO Oxidation," *The Journal of Physical Chemistry C* 125 (2021): 20351–20359.

114. P. Wang, J. Yao, Q. Jiang, et al., "Stabilizing the Isolated Pt Sites on PtGa/Al2O3 Catalyst via Silica Coating Layers for Propane Dehydrogenation at Low Temperature," *Applied Catalysis B: Environmental* 300 (2022): 120731.

115. K. Ding, D. A. Cullen, L. Zhang, et al., "A General Synthesis Approach for Supported Bimetallic Nanoparticles via Surface Inorganometallic Chemistry," *Science* 362 (2018): 560–564.

116. D. Mei, J. H. Kwak, J. Hu, et al., "Unique Role of Anchoring Penta-Coordinated Al 3+ Sites in the Sintering of γ-Al 2 O 3 -Supported Pt Catalysts," *The Journal of Physical Chemistry Letters* 1 (2010): 2688–2691.

117. W.-Z. Jiao, P. Yin, L. Tong, et al., "Pentacoordinate Al 3+ Sites Anchoring Synthesis of Palladium Intermetallic Catalysts on Al 2 O 3 Supports," *Inorganic Chemistry* 61 (2022):6706–6710.

118. J. H. Kwak, J. Hu, D. Mei, et al., "Coordinatively Unsaturated Al 3+ Centers as Binding Sites for Active Catalyst Phases of Platinum on γ-Al 2 O 3," *Science* 325 (2009): 1670–1673.

119. C. Qiu, Y. Odarchenko, Q. Meng, et al., "Direct Observation of the Evolving Metal–support Interaction of Individual Cobalt Nanoparticles at the Titania and Silica Interface," *Chemical Science* 11 (2020): 13060–13070.

120. J. Matos, L. K. Ono, F. Behafarid, et al., "In Situ Coarsening Study of Inverse Micelle-prepared Pt Nanoparticles Supported on γ-Al2O3: Pretreatment and Environmental Effects," *Physical Chemistry Chemical Physics* 14 (2012): 11457.

121. G. J. Kim, D. W. Kwon, and S. C. Hong, "Effect of Pt Particle Size and Valence State on the Performance of Pt/TiO 2 Catalysts for CO Oxidation at Room Temperature," *The Journal of Physical Chemistry C* 120 (2016): 17996–18004.

122. A. Bruix, J. A. Rodriguez, P. J. Ramírez, et al., "A New Type of Strong Metal–Support Interaction and the Production of H 2 through the Transformation of Water on Pt/CeO 2 (111) and Pt/CeO X/TiO 2 (110) Catalysts," *Journal of the American Chemical Society* 134 (2012): 8968–8974.

123. C. T. Campbell, "Electronic Perturbations," *Nature Chemistry* 4 (2012): 597–598.

124. Y. Lykhach, S. M. Kozlov, T. Skála, et al., "Counting Electrons on Supported Nanoparticles," *Nature Materials* 15 (2016): 284–288.

125. T. Ioannides and X. E. Verykios, "Charge Transfer in Metal Catalysts Supported on Doped TiO2: a Theoretical Approach Based on Metal–Semiconductor Contact Theory," *Journal of Catalysis* 161 (1996): 560–569.

126. X. Li, J. Lin, L. Li, et al., "Controlling CO 2 Hydrogenation Selectivity by Metal-Supported Electron Transfer," *Angewandte Chemie International Edition* 59 (2020): 19983–19989.

127. X. Liu, M.-H. Liu, Y.-C. Luo, et al., "Strong Metal–Support Interactions between Gold Nanoparticles and ZnO Nanorods in CO Oxidation," *Journal of the American Chemical Society* 134 (2012): 10251–10258.

128. X. Du, Y. Huang, X. Pan, et al., "Size-dependent Strong Metal-support Interaction in TiO2 Supported Au Nanocatalysts," *Nature Communications* 11 (2020): 5811.

129. X. Wu, C. Liu, H. Wang, Q. Ge, and X. Zhu, "Origin of Strong Metal-support Interactions between Pt and Anatase TiO2 Facets for Hydrodeoxygenation of M-cresol on Pt/TiO2 Catalysts," *Journal of Catalysis* 418 (2023): 203–215.

130. Y. Zhang, J. Liu, K. Qian, et al., "Structure Sensitivity of Au-TiO 2 Strong Metal–Support Interactions," *Angewandte Chemie International Edition* 60 (2021): 12074–12081.

131. S.-I. Ito, T. Fujimori, K. Nagashima, K. Yuzaki, and K. Kunimori, "Strong Rhodium–niobia Interaction in Rh/Nb2O5, Nb2O5–Rh/SiO2 and RhNbO4/SiO2 Catalysts," *Catalysis Today* 57 (2000): 247–254.

132. Z. Majzik, N. Balázs, and A. Berkó, "Ordered SMSI Decoration Layer on Rh Nanoparticles Grown on TiO 2 (110) Surface," *The Journal of Physical Chemistry C* 115 (2011): 9535–9544.

133. J. Li, L. Zhang, X. An, et al., "Tuning Adsorbate-Mediated Strong Metal-Support Interaction by Oxygen Vacancy: a Case Study in Ru/TiO 2," *Angewandte Chemie International Edition* 63 (2024): 202407025.

134. J. Dai, Y. Sun, Z. Liu, Y. Zhang, S. Duan, and R. Wang, *Angewandte Chemie International Edition* 136 (2024): 202409673.

135. H. Wang, Z. Gao, B. Sun, et al., *Chem Catal* 3 (2023): 100768.

136. H. Wang, L. Wang, and F.-S. Xiao, "New Routes for the Construction of Strong Metal—Support Interactions," *Science China Chemistry* 65 (2022): 2051–2057.

137. H. Chen, Z. Yang, X. Wang, et al., "Photoinduced Strong Metal–Support Interaction for Enhanced Catalysis," *Journal of the American Chemical Society* 143 (2021): 8521–8526.

138. J. Zhang, D. Zhu, J. Yan, and C.-A. Wang, *Nature Communications* 12 (2021): 6665.

139. W. Zhang, H. Lin, Y. An, T. Lin, and L. Zhong, *Chemcatchem* 16 (2024): 202301623.

140. G. Wu, Y. Liu, and J. Wang, "Oxidative-Atmosphere-Induced Strong Metal–Support Interaction and Its Catalytic Application," *Accounts of Chemical Research* 56 (2023): 911–923.

141. J. Kim, J. Guo, N. Shan, et al., "Deciphering Catalyst–Support Interaction via Doping for Highly Active and Durable Oxygen Evolution Catalysis," *Journal of the American Chemical Society* 147 (2025): 16340–16349.

142. X. Wang, X. Yang, G. Pei, et al., "Strong Metal–support Interaction Boosts the Electrocatalytic Hydrogen Evolution Capability of Ru Nanoparticles Supported on Titanium Nitride," *Carbon Energy* 6 (2024): 391.

143. Z. Wang, Z. Mei, L. Wang, et al., "Insight into the Activity of Ni-based Thermal Catalysts for Dry Reforming of Methane," *Journal of Materials Chemistry A* 12 (2024): 24802–24838.

144. Y. Gangarajula, F. Hong, Q. Li, et al., "Operando Induced Strong Metal-support Interaction of Rh/CeO2 Catalyst in Dry Reforming of Methane," *Applied Catalysis B: Environmental* 343 (2024): 123503.

145. S. Bernal, J. J. Calvino, M. A. Cauqui, et al., "Some Contributions of Electron Microscopy to the Characterisation of the Strong Metal–support Interaction Effect," *Catalysis Today* 77 (2003): 385.

146. Z. Sun, W. Shi, L. R. Smith, et al., "Concerted Catalysis of Single Atom and Nanocluster Enhances Bio-ethanol Activation and Dehydrogenation," *Nature Communications* 16 (2025): 3935.

147. B. Liu, M. Li, X. Chen, et al., *Journal of the American Chemical Society* 147 (2025): 15895.

148. L. Zhang, J. Yu, X. Sun, and J. Sun, *Journal of CO2 Utilization* 71 (2023): 102460.

149. M. Tang, S. Li, S. Chen, et al., "Facet-Dependent Oxidative Strong Metal-Support Interactions of Palladium–TiO 2 Determined by in Situ Transmission Electron Microscopy," *Angewandte Chemie International Edition* 60 (2021): 22339–22344.

150. S. Jin, Z. Zhang, D. Li, Y. Wang, C. Lian, and M. Zhu, "Alcohol-Induced Strong Metal-Support Interactions in a Supported Copper/ZnO Catalyst," *Angewandte Chemie International Edition* 62 (2023): 202301563.

151. Y. Sang, J. Wang, M. Xu, et al., "Engineering Robust Hydrophilic–Hydrophobic Interface via π-Electron Delocalization for Ultralong-Lived Zinc–Ion Batteries," *Angewandte Chemie* 137 (2025): 202506984.

152. Z. Mei, T. Li, J. Zhou, et al., *Chemcatchem* 17 (2025): 202500583.

153. M. Su, H. Dou, J. Yan, et al., "Multisite Cooperative Regulation of Solvation and Interface via Dynamic Additive Engineering for Highly Reversible Zinc Batteries," *Angewandte Chemie International Edition* 64 (2025): 202511685.

154. A. Han, X. Zhou, X. Wang, et al., *Nature Communications* 12 (2021): 709.

155. Z. Wang, D. Shu, H. Chen, et al., "Dynamic Interplay between Particle Size and Strong Metal Support Interaction in Rh/TiO 2 Tuning the Selectivity of CO 2 Hydrogenation," *ACS Catalysis* 15 (2025): 4101–4109.

156. A. C. Foucher, N. Marcella, J. D. Lee, et al., "Structural and Valence State Modification of Cobalt in CoPt Nanocatalysts in Redox Conditions," *ACS Nano* 15 (2021): 20619–20632.

157. Y. Ding, H. Wang, B. Huang, Y. Chang, Y. Hua, and Z. Qu, "Controlled Growth of Silver Nanoparticles by Metal–Support Interaction for Enhanced Tandem Catalytic Oxidation of HCHO at Low Temperature," *ACS Catalysis* 15 (2025): 1411–1421.

158. J. Abed, J. Heras-Domingo, R. Y. Sanspeur, et al., "Pourbaix Machine Learning Framework Identifies Acidic Water Oxidation Catalysts Exhibiting Suppressed Ruthenium Dissolution," *Journal of the American Chemical Society* 146 (2024): 15740–15750.

159. A. K. Singh, N. K. Pande, and A. T. Bell, "Electron Microscopy Study of the Interactions of Rhodium with Titania," *Journal of Catalysis* 94 (1985): 422–435.

160. A. D. Logan, E. J. Braunschweig, A. K. Datye, and D. J. Smith, "Direct Observation of the Surfaces of Small Metal Crystallites: Rhodium Supported on Titania," *Langmuir* 4 (1988): 827–830.

161. D. Laudenschleger, H. Ruland, and M. Muhler, "Identifying the Nature of the Active Sites in Methanol Synthesis over Cu/ZnO/Al2O3 Catalysts," *Nature Communications* 11 (2020): 3898.

162. S. Kattel, P. J. Ramírez, J. G. Chen, J. A. Rodriguez, and P. Liu, "Active Sites for CO 2 Hydrogenation to Methanol on Cu/ZnO Catalysts," *Science* 355 (2017): 1296–1299.

163. F. (Feng) Tao and P. A. Crozier, "Atomic-Scale Observations of Catalyst Structures under Reaction Conditions and during Catalysis," *Chemical Reviews* 2016, 116, 3487.

164. Y. Zhou, C. Jin, Y. Li, and W. Shen, "Dynamic Behavior of Metal Nanoparticles for Catalysis," *Nano Today* 20 (2018): 101–120.

165. X. Sun, W. Zhu, D. Wu, et al., "Surface-reaction Induced Structural Oscillations in the Subsurface," *Nature Communications* 11 (2020): 305.

166. L. Piccolo, "Restructuring Effects of the Chemical Environment in Metal Nanocatalysis and Single-atom Catalysis," *Catalysis Today* 373 (2021): 80–97.

167. P. L. Hansen, J. B. Wagner, S. Helveg, J. R. Rostrup-Nielsen, B. S. Clausen, and H. Topsøe, "Atom-Resolved Imaging of Dynamic Shape Changes in Supported Copper Nanocrystals," *Science* 295 (2002): 2053–2055.

168. H. Yoshida, Y. Kuwauchi, J. R. Jinschek, et al., "Visualizing Gas Molecules Interacting with Supported Nanoparticulate Catalysts at Reaction Conditions," *Science* 335 (2012): 317–319.

169. Q.-Y. Fan, F.-Q. Gong, Y.-P. Liu, H.-X. Zhu, and J. Cheng, "Modeling Dynamic Catalysis at Ab Initio Accuracy: the Need for Free-Energy Calculation," *ACS Catalysis* 14 (2024): 16086–16097.

170. D. M. Foster, T. Pavloudis, J. Kioseoglou, and R. E. Palmer, "Atomic-resolution Imaging of Surface and Core Melting in Individual Size-selected Au Nanoclusters on Carbon," *Nature Communications* 10 (2019): 2583.

171. T. Pu, J. Chen, W. Tu, et al., "Dependency of CO2 Methanation on the Strong Metal-support Interaction for Supported Ni/CeO2 Catalysts," *Journal of Catalysis* 413 (2022): 821–828.

172. L. Liu, D. N. Zakharov, R. Arenal, P. Concepcion, E. A. Stach, and A. Corma, "Evolution and Stabilization of Subnanometric Metal Species in Confined Space by in Situ TEM," *Nature Communications* 9 (2018): 574.

173. M. Moliner, J. E. Gabay, C. E. Kliewer, et al., "Reversible Transformation of Pt Nanoparticles into Single Atoms inside High-Silica Chabazite Zeolite," *Journal of the American Chemical Society* 138 (2016): 15743–15750.

174. L. Liu, U. Díaz, R. Arenal, G. Agostini, P. Concepción, and A. Corma, "Generation of Subnanometric Platinum with High Stability during Transformation of a 2D Zeolite into 3D," *Nature Materials* 16 (2017): 132–138.

175. R. Ishikawa, T. Futazuka, Y. Jimbo, K. Kawahara, N. Shibata, and Y. Ikuhara, "Real-time Tracking of Three-dimensional Atomic Dynamics of Pt Trimer on TiO 2 (110)," *Science Advances* 10 (2024): adk6501.

176. L. Liu, D. M. Meira, R. Arenal, P. Concepcion, A. V. Puga, and A. Corma, "Determination of the Evolution of Heterogeneous Single Metal Atoms and Nanoclusters under Reaction Conditions: Which Are the Working Catalytic Sites?," *ACS Catalysis* 9 (2019): 10626–10639.

177. L. Liu, M. Lopez-Haro, C. W. Lopes, et al., "Structural Modulation and Direct Measurement of Subnanometric Bimetallic PtSn Clusters Confined in Zeolites," *Nature Catalysis* 3 (2020): 628–638.

178. L. Liu, M. Lopez-Haro, C. W. Lopes, et al., "Atomic-level Understanding on the Evolution Behavior of Subnanometric Pt and Sn Species during High-temperature Treatments for Generation of Dense PtSn Clusters in Zeolites," *Journal of Catalysis* 391 (2020): 11–24.

179. W. Gui, S. Jiang, L. Wang, et al., "Construction of Asymmetric Anion Layer to Accelerate Carrier Reaction Kinetics and Thermodynamically Promote Photocatalytic CO 2 Reduction," *Advanced Functional Materials* 35 (2025): 2505919.

180. S. Li, X. Li, Y. Liang, et al., "Full-Lifecycle Biocarbon Foam through Multiscale Pore Engineering toward Ultra-High Electromagnetic Absorption," *Advanced Functional Materials* (2025): 13375.

181. Y.-X. Zhu and G.-C. Wang, "Mechanism Exploration of the Water–Gas Shift Reaction on Cu 4/CeO 2 (110) under Realistic Reaction Temperatures," *The Journal of Physical Chemistry C* 129 (2025): 4985–4997.

182. O. Mohan, Shambhawi, A. A. Lapkin, and S. H. Mushrif, "Investigating Methane Dry Reforming on Ni and B Promoted Ni Surfaces: DFT Assisted Microkinetic Analysis and Addressing the Coking Problem," *Catalysis Science & Technology* 10 (2020): 6628–6643.

183. M. García-Mota, M. Bajdich, V. Viswanathan, A. Vojvodic, A. T. Bell, and J. K. Nørskov, "Importance of Correlation in Determining Electrocatalytic Oxygen Evolution Activity on Cobalt Oxides," *The Journal of Physical Chemistry C* 116 (2012): 21077–21082.

184. Z. Tang, Y. Li, K. Zhang, et al., "Interfacial Hydrogen Spillover on Pd-TiO 2 with Oxygen Vacancies Promotes Formate Electrooxidation," *ACS Energy Letters* 8 (2023): 3945–3954.

185. Z. Guo, Y. Yu, C. Li, et al., "Deciphering Structure-Activity Relationship toward CO 2 Electroreduction over SnO 2 by a Standard Research Paradigm," *Angewandte Chemie International Edition* 63 (2024): 202319913.

186. Y. Sun, S. Sun, Y. Zheng, et al., "The Role of Oxygen Vacancies on SnO2 in Improving Formaldehyde Competitive Adsorption: a DFT Study with an Experimental Verification," *Applied Surface Science* 570 (2021): 151110.

187. X. Yan, C. Duan, S. Yu, B. Dai, C. Sun, and H. Chu, *Journal of CO2 Utilization* 2024, 79, 102648.

188. R. Fan, Y. Zhang, Z. Hu, et al., "Synergistic Catalysis of Cluster and Atomic Copper Induced by Copper-silica Interface in Transfer-hydrogenation," *Nano Research* 14 (2021): 4601–4609.

189. G. Sun, A. N. Alexandrova, and P. Sautet, "Pt8 cluster on Alumina under a Pressure of Hydrogen: Support-dependent Reconstruction from First-principles Global Optimization," *The Journal of Chemical Physics* 151 (2019): 194703.

190. H. Zhai and A. N. Alexandrova, "Ensemble-Average Representation of Pt Clusters in Conditions of Catalysis Accessed through GPU Accelerated Deep Neural Network Fitting Global Optimization," *Journal of Chemical Theory and Computation* 12 (2016): 6213–6226.

191. J.-J. Sun and J. Cheng, "Solid-to-liquid Phase Transitions of Subnanometer Clusters Enhance Chemical Transformation," *Nature Communications* 10 (2019): 5400.

192. Q.-Y. Fan, J.-J. Sun, F. Wang, and J. Cheng, "Adsorption-Induced Liquid-to-Solid Phase Transition of Cu Clusters in Catalytic Dissociation of CO 2," *The Journal of Physical Chemistry Letters* 11 (2020): 7954–7959.

193. Y. He, J.-C. Liu, L. Luo, et al., "Size-dependent Dynamic Structures of Supported Gold Nanoparticles in CO Oxidation Reaction Condition," *Proceedings of the National Academy of Sciences* 115 (2018): 7700–7705.

194. R. Y. Brogaard, M. Kømurcu, M. M. Dyballa, et al., "Ethene Dimerization on Zeolite-Hosted Ni Ions: Reversible Mobilization of the Active Site," *ACS Catalysis* 9 (2019): 5645–5650.

195. V. Van Speybroeck, M. Bocus, P. Cnudde, and L. Vanduyfhuys, "Operando Modeling of Zeolite-Catalyzed Reactions Using First-Principles Molecular Dynamics Simulations," *ACS Catalysis* 13 (2023): 11455–11493.

196. X. Liu and D. R. Salahub, "Molybdenum Carbide Nanocatalysts at Work in the in Situ Environment: a Density Functional Tight-Binding and Quantum Mechanical/Molecular Mechanical Study," *Journal of the American Chemical Society* 137 (2015): 4249–4259.

197. X. Guan, J. P. Heindel, T. Ko, C. Yang, and T. Head-Gordon, "Using Machine Learning to Go beyond Potential Energy Surface Benchmarking for Chemical Reactivity," *Nature Computational Science* 3 (2023): 965–974.

198. F.-Q. Gong, Y.-P. Liu, Y. Wang, W. E, Z.-Q. Tian, and J. Cheng, "Machine Learning Molecular Dynamics Shows Anomalous Entropic Effect on Catalysis through Surface Pre-Melting of Nanoclusters," *Angewandte Chemie International Edition* 63 (2024): 202405379.

199. F. Wang, Y. Sun, and J. Cheng, "Switching of Redox Levels Leads to High Reductive Stability in Water-in-Salt Electrolytes," *Journal of the American Chemical Society* 145 (2023): 4056–4064.

200. Y.-G. Wang, Y. Yoon, V.-A. Glezakou, J. Li, and R. Rousseau, "The Role of Reducible Oxide–Metal Cluster Charge Transfer in Catalytic Processes: New Insights on the Catalytic Mechanism of CO Oxidation on Au/TiO 2 from Ab Initio Molecular Dynamics," *Journal of the American Chemical Society* 135 (2013): 10673–10683.

201. Z. W. Ulissi, A. J. Medford, T. Bligaard, and J. K. Nørskov, "To Address Surface Reaction Network Complexity Using Scaling Relations Machine Learning and DFT Calculations," *Nature Communications* 8 (2017): 14621.

202. F. Wang, Z. Ma, and J. Cheng, "Accelerating Computation of Acidity Constants and Redox Potentials for Aqueous Organic Redox Flow Batteries by Machine Learning Potential-Based Molecular Dynamics," *Journal of the American Chemical Society* 146 (2024): 14566–14575.

203. J. T. Margraf, H. Jung, C. Scheurer, and K. Reuter, "Exploring Catalytic Reaction Networks with Machine Learning," *Nature Catalysis* 6 (2023): 112–121.

204. C. M. Handley and P. L. Popelier, "Potential Energy Surfaces Fitted by Artificial Neural Networks," *The Journal of Physical Chemistry A* 114 (2010): 3371–3383.

205. J. Behler, "Neural Network Potential-energy Surfaces in Chemistry: a Tool for Large-scale Simulations," *Physical Chemistry Chemical Physics* 13 (2011): 17930.

206. J. Behler and G. Csányi, "Machine Learning Potentials for Extended Systems: a Perspective," *The European Physical Journal B* 94 (2021): 142.

207. Q. Yu, R. Ma, C. Qu, et al., "Extending Atomic Decomposition and Many-body Representation with a Chemistry-motivated Approach to Machine Learning Potentials," *Nature Computational Science* 5 (2025): 418–426.

208. T. Mou, H. S. Pillai, S. Wang, et al., "Bridging the Complexity Gap in Computational Heterogeneous Catalysis with Machine Learning," *Nature Catalysis* 6 (2023): 122–136.

209. M. L. Paleico and J. Behler, "Global Optimization of Copper Clusters at the ZnO(101¯0) Surface Using a DFT-based Neural Network Potential and Genetic Algorithms," *The Journal of Chemical Physics* 153 (2020): 054704.

210. J. S. Elias, N. Artrith, M. Bugnet, et al., "Elucidating the Nature of the Active Phase in Copper/Ceria Catalysts for CO Oxidation," *ACS Catalysis* 6 (2016): 1675–1679.

211. F.-Q. Gong, Y.-P. Liu, Y. Wang, W. E, Z.-Q. Tian, and J. Cheng, "Machine Learning Molecular Dynamics Shows Anomalous Entropic Effect on Catalysis through Surface Pre-Melting of Nanoclusters," *Angewandte Chemie International Edition* 63 (2024): 202405379.

212. L. Zhou, P. Fu, R. Wang, et al., "Dynamic Phase Transitions Dictate the Size Effect and Activity of Supported Gold Catalysts," *Science Advances* 10 (2024): 4145.

213. W. Shu, J. Li, J.-X. Liu, et al., "Structure Sensitivity of Metal Catalysts Revealed by Interpretable Machine Learning and First-Principles Calculations," *Journal of the American Chemical Society* 146 (2024): 8737–8745.

214. J. Xu, X.-M. Cao, and P. Hu, "Improved Prediction for the Methane Activation Mechanism on Rutile Metal Oxides by a Machine Learning Model with Geometrical Descriptors," *The Journal of Physical Chemistry C* 123 (2019): 28802–28810.

215. A. R. Singh, B. A. Rohr, J. A. Gauthier, and J. K. Nørskov, "Predicting Chemical Reaction Barriers with a Machine Learning Model," *Catalysis Letters* 149 (2019): 2347–2354.

216. T. Song, M. Luo, X. Zhang, et al., "A Multiagent-Driven Robotic AI Chemist Enabling Autonomous Chemical Research on Demand," *Journal of the American Chemical Society* 147 (2025): 12534–12545.

217. Q. Zhu, Y. Huang, D. Zhou, et al., "Automated Synthesis of Oxygen-producing Catalysts from Martian Meteorites by a Robotic AI Chemist," *Nature Synthesis* 3 (2024): 319–328.

218. Q. Zhu, F. Zhang, Y. Huang, et al., "An All-round AI-Chemist with a Scientific Mind," *National Science Review* 9 (2022): nwac190.